ChemPubSoc Europe

DOI: 10.1002/cbic.201600048

CHEMBIOCHEM Full Papers

Synthesis and Kinetic Characterisation of Water-Soluble Fluorogenic Acyl Donors for Transglutaminase 2

Robert Wodtke,[a, c] Georg Schramm,[a, d] Jens Pietzsch,[a, c] Markus Pietsch,*[b] and Reik Löser*[a, c]

Small glutamate-containing peptides bearing coumarin derivatives as fluorescent leaving groups attached to the γ-carboxylic acid group of the Glu residue were synthesised and investigated with regard to their potential to act as substrates for transglutaminase 2 (TGase 2). Their synthesis was accomplished by an efficient solid-phase approach. The excellent water solubility of the compounds enabled their extensive kinetic characterisation in the context of TGase 2-catalysed hydrolysis and aminolysis. The influence of the coumarin skeleton's substitution pattern on the kinetic properties was studied. Derivatives containing 7-hydroxy-4-methylcoumarin (HMC) revealed properties superior to those of their 7-hydroxycoumarin counterparts; analogous amides are not accepted as substrates. Z-Glu(HMC)-Gly-OH, which exhibited the best substrate properties out of the investigated derivatives, was selected for representative kinetic characterisation of acyl acceptor substrates and irreversible inhibitors.

Introduction

The quantitative determination of enzyme activities is of outstanding importance in biochemical research. Enzymatic assays provide the basis for the functional characterisation of enzymes in terms of kinetic parameters and are crucial for studying these biocatalysts in their biological contexts. In the field of drug discovery, the availability of methods that allow assaying of enzymes is a prerequisite for the identification and characterisation of inhibitors. In addition, the development of substrate-based probes that can efficiently monitor enzymes for diagnostic or imaging purposes requires their evaluation on the basis of kinetic properties. To facilitate sensitive and facile quantification, enzyme substrates should contain moieties that are released upon conversion and can be reliably detected by spectroscopic methods/analytical instruments. Enzymes that catalyse the transfer of acyl moieties to water or to alternative nucleophiles—such as hydrolases or acyl transferases—often accept chromophores or fluorophores as leaving groups within the acyl donor substrate. When these chromophores or fluorophores contain electron-donating groups, such as OH or NH_2, attachment of acyl residues to these groups usually results in attenuation of the absorption and emission intensities. Upon enzyme-catalysed cleavage, the spectroscopic properties are restored, and this thus couples enzymatic activity to signal increase.[1]

Transglutaminases are acyl transferases of particular importance. Among them, transglutaminase 2 (TGase 2, tissue transglutaminase) seems to be most obviously involved in human disease progression. TGase 2 is a ubiquitously occurring enzyme in mammals, exhibiting several important biological functions.[2] The eponymous and best-characterised role is its function as a Ca^{2+}-dependent catalyst of acyl transfer between protein-bound glutamine residues and primary amines, particularly protein-bound lysine residues and low-molecular-weight polyamines.[3] In addition to catalysing such transamidation reactions, TGase 2 is able to hydrolyse the γ-carboxamide group of a glutamine residue, thus generating a glutamate residue.[4]

The acyl transferase activity of TGase 2 is considered to be latent under physiological conditions, but rapid activation occurs in stress situations, such as apoptosis, in which cross-linking of proteins stabilises dying cells.[5] In the course of TGase 2 research, further diverse enzymatic and non-enzymatic functions that might be more relevant under physiological conditions for maintaining the integrity of the cell have been ascribed to this enzyme.[6]

TGase 2, particularly its acyl transferase activity, contributes to different pathophysiological conditions, such as celiac disease,[7] diseases related to fibrotic processes,[8] neurodegenerative disorders[9] and cancer.[10] Therefore, this enzyme appears to be an attractive target for pharmacological inhibition to po-

[a] R. Wodtke, Dr. G. Schramm, Prof. Dr. J. Pietzsch, Dr. R. Löser
Helmholtz-Zentrum Dresden–Rossendorf
Institut für Radiopharmazeutische Krebsforschung
Bautzner Landstrasse 400, 01328 Dresden (Germany)
E-mail: r.loeser@hzdr.de

[b] Dr. M. Pietsch
Zentrum für Pharmakologie, Medizinische Fakultät, Universität zu Köln
Gleueler Strasse 24, 50931 Köln (Germany)
E-mail: markus.pietsch@uk-koeln.de

[c] R. Wodtke, Prof. Dr. J. Pietzsch, Dr. R. Löser
Fachrichtung Chemie und Lebensmittelchemie
Technische Universität Dresden
Mommsenstrasse 4, 01062 Dresden (Germany)

[d] Dr. G. Schramm
Present address: Department of Imaging and Pathology, KU Leuven
UZ Herestraat 49, 3000 Leuven (Belgium)

Supporting information for this article can be found under http://dx.doi.org/10.1002/cbic.201600048.

tentially treat these diseases. In addition, the development of imaging agents targeted against TGase 2 should provide further insight into its pathological functions and should support clinical translation of inhibitors.

One of the prerequisites for the development of TGase 2 inhibitors is the availability of reliable assay methods for precise measurement of the enzymatic activity, which should enable the evaluation of the compounds' inhibitory potencies. Various continuous and discontinuous assay methods for TGase 2 have been described so far and were recently discussed in detail.[11] Among these assay methods, the continuous fluorimetric activity assay described by Gillet et al.[12] seems to be highly suitable for inhibitor characterisation because it allows for the sensitive detection of TGase 2 activity by measurement of increases in fluorescence (Scheme 1).

Synthetic access to the required fluorogenic acyl donors, each consisting of a Z-protected amino acid [Z: benzyloxycarbonyl, also referred to as carbobenzoxy (Cbz) group] connected to umbelliferone (7-hydroxycoumarin, HC) through a γ-aminobutyroyl (γ-Abu) linker acting as mimetic of the glutamine side chain, is fairly easy. In addition, the assay allows for the kinetic characterisation both of inhibitors and of acyl acceptor substrates. Therefore, we set out to establish this fluorimetric assay in our laboratories by using the fluorogenic acyl donor Z-Phe-γ-Abu-HC. However, as outlined later in this article, both Z-Phe-γ-Abu-HC and its 7-hydroxy-4-methylcoumarin-based (HMC-based) derivative proved to have the disadvantage of low solubility in aqueous media. Depending on the experimental setup, this might limit the applicability of these compounds for detailed kinetic studies, because such investigations require activity measurements over a broad range of substrate concentrations. In particular, simultaneous measurements of various substrate concentrations in a microplate format can be more affected by solubility limits than single measurements in a cuvette,[12] due to the different time delays caused by preparation.

We therefore set out to develop analogues with improved solubility. A general approach to making compounds more soluble in water is the attachment of ionisable functionalities such as carboxylic acid groups.[13] Applied to the TGase 2 substrates discussed above, such derivatisation seems to be most easily achievable by replacing the γ-aminobutyroyl moiety with glutamate.

Here we describe the synthesis and kinetic characterisation of six new glutamate-derived fluorogenic acyl donors. A solid-phase synthesis strategy was developed for this purpose, and the compounds were evaluated in terms of their enzymatic hydrolysis and aminolysis, both by standard regression analysis and by numerical integration. Together with investigations into different peptidic scaffolds for recognition by TGase 2, the influence of substitutions on the fluorophore was explored. Because all compounds exhibit distinct rates of spontaneous reactions, this feature was in turn used to assess their solubilities. In addition to the coumarinyl esters, two coumarinyl amides were synthesised in order to determine their potential to act as fluorogenic acyl donors. Furthermore, the applicability of the new acyl donors for kinetic characterisation of amine-based acyl acceptor substrates [aminoacetonitrile and *N*-(biotinyl)cadaverine] and irreversible inhibitors [iodoacetamide and the recently described N^{α}-phenylacetyl-N^{ε}-acryloyl-lysine-4-(6-methylpyridine-2-yl)piperazide[14]] was verified.

Results and Discussion

Synthesis and kinetic evaluation of the γ-Abu-derived acyl donors

Initially, it was envisaged that a fluorimetric activity assay for TGase 2 could be established by using the acyl donors described by Gillet et al.[12] Because the reported kinetic data were more favourable for *Z*-Phe-γ-Abu-HC (**2a**) than for its glycine derivative *Z*-Gly-γ-Abu-HC, we focused on the former compound. Moreover, other coumarin derivatives—that is, HMC and 7-amino-4-methylcoumarin (AMC)—were employed as fluorogenic leaving groups. The syntheses of these three compounds were each accomplished in two steps by the published procedure with some modifications, starting from commercially available Z-Phe-OH (Scheme 2 and Discussion S1 in the Supporting Information for detailed experimental procedures).[12] After purification by column chromatography and recrystallisation, the fluorogenic acyl donors **2a**–**2c** were obtained in satisfactory yields (55–68%) and high purities.

Initial investigations were focussed on the enzymatic aminolysis of the acyl donors **2a** and **2b** at pH 8.0 with aminoacetonitrile as acyl acceptor in the presence of (±)-*threo*-dithiothreitol (DTT) as antioxidant. As in the reported assay procedure,

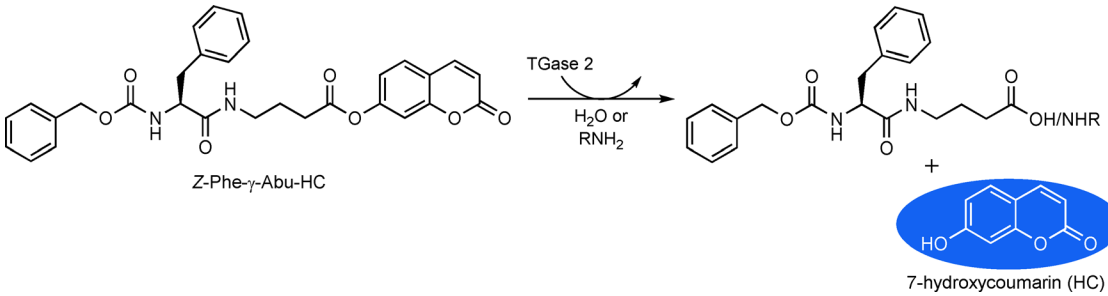

Scheme 1. Principle of the fluorimetric TGase 2 activity assay developed by Gillet et al.[12] Release of 7-hydroxycoumarin (HC) by TGase 2-catalysed hydrolysis or aminolysis of Z-Phe-γ-Abu-HC results in a measureable increase in fluorescence.

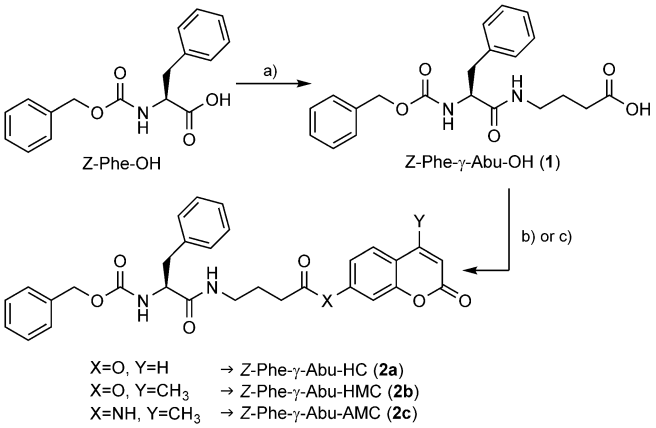

Scheme 2. Synthesis of the γ-aminobutyric acid-derived fluorogenic acyl donors **2a**–**2c**. Reagents and conditions: a) *N*-methylmorpholine (NMM), isobutyl chloroformate (IBCF), γ-Abu-OH, aqueous NaOH, THF, −30→10 °C, 2.5 h; b) HC/HMC, *N*,*N*-dicyclohexylcarbodiimide (DCC), 4-(dimethylamino)-pyridine (DMAP), CH_2Cl_2/THF (4:1), 25 h; c) AMC, NMM, IBCF, THF/DMF (12:1), −25 °C→10 °C, 5 h.

a final concentration of 5% DMF or DMSO was used to achieve sufficient solubility of the acyl donors in aqueous media.[12] The increase in fluorescence was monitored in 96-well microplates at different concentrations of **2a** (5–40 μM) and **2b** (1–20 μM), and initial rates ($v_{0\,total}$) were calculated as outlined in the Experimental Section. Unexpectedly, plots of $v_{0\,total}$ versus the acyl donor concentration for both compounds each exhibited a maximum at ≈5 μM, after which the rates suddenly dropped and further increased with rising substrate concentrations (Figure S1). Concomitantly, visual inspection of plate wells revealed the formation of precipitates even at acyl donor concentrations below 20 μM, independently of the organic co-solvent used.

This observation suggested that the anomalous Michaelis–Menten plots are caused by limited solubility of **2a** and **2b**. Generally, a poorly soluble substrate will follow the Michaelis–Menten hyperbola only up to the solubility limit without reaching V_{max}, "since the concentration of substrate which saturates an aqueous solution is insufficient to saturate the enzyme".[15]

To investigate the solubility behaviour of the acyl donors in more detail, we decided to take advantage of their spontaneous decay that takes place in the absence of TGase 2 and aminoacetonitrile. Because these reactions each follow pseudo-first-order kinetics, plots of initial rates ($v_{0\,control}$) versus concentration should display a linear dependence in the case of complete solubility.[16] The results of this investigation confirmed the initial observations on the low solubilities of the γ-Abu-derived acyl donors, because the curves deviated from linearity even at low concentrations (< 15 μM, Figure S2) before precipitation could be observed visually, thus indicating aggregation prior to precipitate formation. Moreover, as shown in Figure S2, the solubilities of the two γ-Abu derivatives are highly time dependent and strongly influenced both by the organic co-solvent and by the antioxidant present.

However, to demonstrate their potential as substrates, compounds **2a** and **2b** were evaluated in terms of gpTGase 2-catalysed hydrolysis within their solubility limits (Figure S3). Nonlinear regression according to the Michaelis–Menten equation [Experimental Section, Eq. (4)] revealed K_m and k_{cat} values of 1.47 μM and 0.30 s^{-1}, respectively, for acyl donor **2a** and 1.14 μM and 0.52 s^{-1}, respectively, for acyl donor **2b**, resulting in performance constants of 204000 and 456000 $M^{-1}s^{-1}$, respectively (Table 1). These results clearly confirm the favourable substrate properties of the γ-Abu derivatives.[12] Interestingly, despite similar K_m values, substitution of HC by HMC resulted in a k_{cat} value for acyl donor **2b** almost twice that for **2a**. Because of their low K_m values, both coumarinyl esters can be applied for investigations into the hydrolytic activity of TGase 2 up to concentrations of 3–6×K_m, depending on the buffer conditions used.

In contrast to the coumarinyl esters **2a** and **2b**, neither spontaneous nor enzymatic release of AMC was observed for coumarinyl amide **2c** (data not shown). This is discussed later in this article.

Table 1. Kinetic parameters for the TGase 2-catalysed hydrolyses of the acyl donors **2**–**6** at pH 8.0 and 30 °C.

Compound	Regression analysis			Numerical integration		
	K_m [μM]	k_{cat} [s^{-1}]	k_{cat}/K_m [$M^{-1}s^{-1}$]	K_m [μM]	k_{cat} [s^{-1}]	k_{cat}/K_m [$M^{-1}s^{-1}$]
	gpTGase 2					
2a	1.47 (0.02)	0.30 (0.03)	204000	1.24 (0.06)	0.25 (0.01)	202000
2b	1.14 (0.16)	0.52 (0.03)	456000	1.20 (0.27)	0.46 (0.04)	383000
3	12.1 (0.5)	0.50 (0.01)	41300	10.9 (0.9)	0.43 (0.01)	39500
4	17.7 (0.5)	0.29 (0.03)	16400	12.4 (0.6)	0.23 (0.02)	18500
5a	2.83 (0.17)	0.71 (0.02)	251000	2.57 (0.46)	0.62 (0.02)	241000
5b	2.53 (0.14)	0.76 (0.02)	300000	2.49 (0.23)	0.71 (0.02)	285000
6a	11.0 (0.6)	0.64 (0.03)	58200	8.87 (0.64)	0.55 (0.01)	62000
6b	2.66 (0.11)	0.55 (0.02)	207000	2.14 (0.13)	0.54 (0.02)	252000
	hTGase 2					
5a	12.7 (0.9)	0.84 (0.05)	66100	9.72 (0.62)	0.74 (0.04)	76100
5b	8.62 (0.09)	0.68 (0.02)	78900	6.06 (0.16)	0.64 (0.02)	106000
6b	13.6 (1.3)	0.50 (0.03)	36800	7.73 (0.54)	0.48 (0.03)	62100

For details on calculation of the kinetic parameters see the Experimental Section. Data shown are mean values (±SEMs) of three separate experiments, each performed in duplicate. Active concentrations of TGase 2 from guinea pig liver (E_T = 31.6–35.3 nM, various lots) and human (E_T = 30.8 nM) were calculated from Zedira's activity data or determined by active site titration as recently described,[30] respectively.

Synthesis and spontaneous reactivity of the glutamate-derived acyl donors

To overcome the low solubilities, derivatisation of fluorogenic acyl donors with a carboxylic acid group as a solubilising moiety was envisaged.[13] From a synthetic point of view, the most straightforward way to achieve this seemed to be by replacement of the γ-aminobutyroyl linker that connects Z-Phe and the fluorophore by a glutamoyl moiety, thus resulting in Z-Phe-Glu(fluorophore)-OH as the basic dipeptidic structure. Moreover, this scaffold allows for the C-terminal extension of the scaffold structure by an additional amino acid such as glycine, which would place the solubility-mediating carboxylic acid group further away from the reaction centre.

In order to define the minimal structural motif for efficient TGase 2-catalysed conversion, the effect of deleting the N-terminal Phe moiety had to be studied. Therefore, Z-Glu(fluorophore)-OH, Z-Glu(fluorophore)-Gly-OH and Z-Phe-Glu(fluorophore)-Gly-OH were examined as amino-acid-based and peptidic scaffolds for substrate synthesis in addition to Z-Phe-Glu-(fluorophore)-OH. Because γ-Abu derivative **2b** exhibits more favourable substrate properties than **2a**, HMC was selected as fluorophore for all peptidic scaffolds. However, to investigate the influence of methyl substitution in the coumarin fluorophore on the substrate properties towards TGase 2, HC derivatives of the most favourable peptidic structures Z-Glu-Gly-OH and Z-Phe-Glu-Gly-OH (see Kinetics Section) were also synthesised. Finally, Z-Glu(AMC)-Gly-OH (**5c**) was prepared to ascertain whether or not coumarinyl amides can be used as fluorogenic acyl donors for TGase 2.

A major challenge to the synthesis of the glutamate-derived acyl donors involves the regioselective installation of the fluorogenic leaving group in the side chain of the glutamate residue. Therefore, a strategy based on solid-phase synthesis with use of orthogonal protecting groups was developed to provide the different glutamate-derived acyl donors (Scheme 3). In addition, this modular approach should allow efficient access to a broad spectrum of potential acyl donors. For this purpose, the 2-chlorotrityl chloride (2-ClTrtCl) resin was considered to be the optimal polymeric support because the anchoring moiety readily reacts with carboxylic acid groups, and the corresponding highly acid-labile 2-chlorotrityl esters can be easily cleaved under mildly acidic conditions (see below).[17] Final esterification at the glutamate side chain required careful optimisation with regard to the selection of the coupling reagents (see Discussion S2). It was accordingly found that the use of

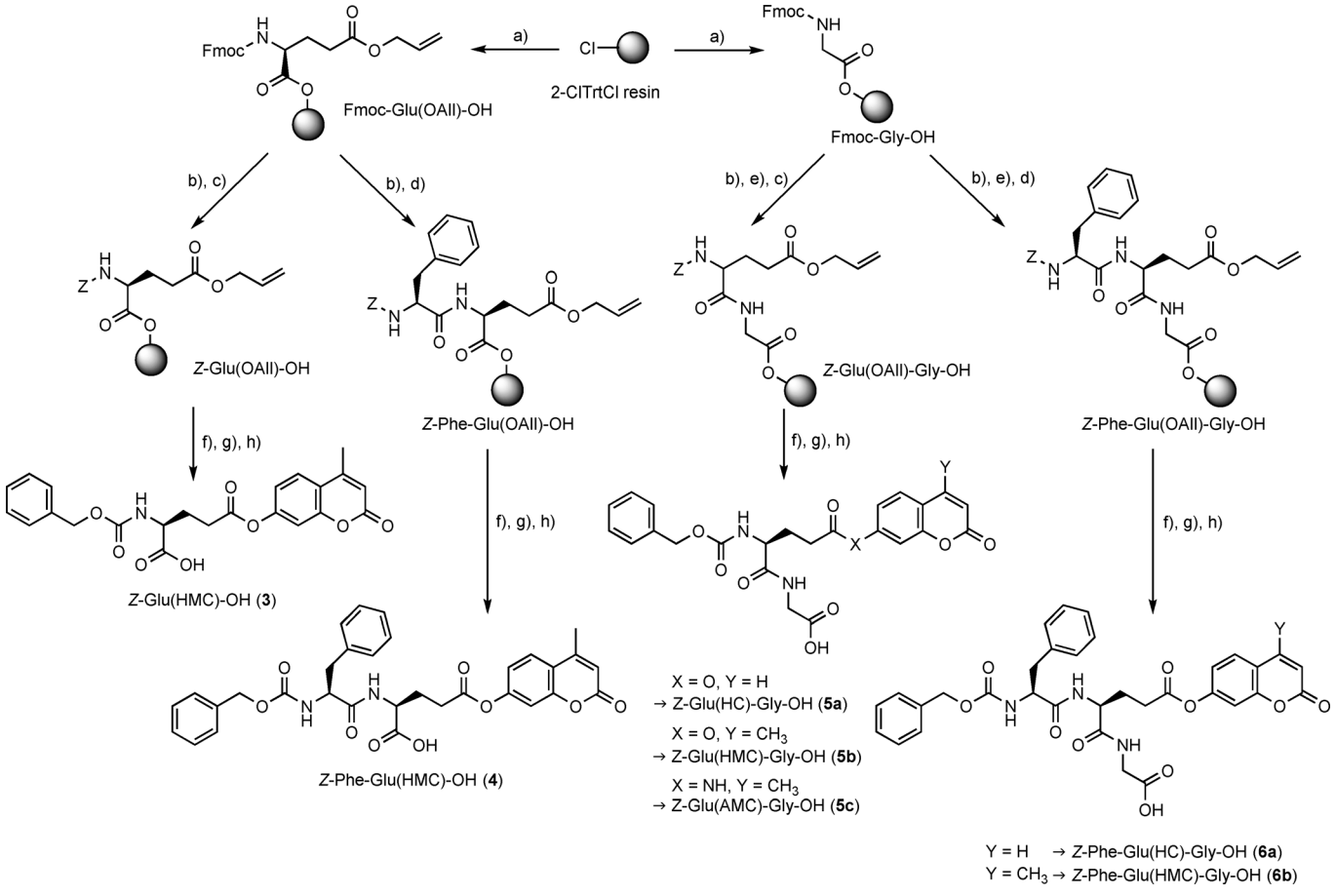

Scheme 3. Solid-phase synthesis of the glutamate-derived fluorogenic acyl donors **3**–**6**. Reagents and conditions: a) 1. Fmoc-AA, DIPEA, CH_2Cl_2, 4 h, 2. CH_2Cl_2/CH_3OH/DIPEA (17:1:2); b) 20% piperidine/DMF; c) Z-OSu, DIPEA, CH_2Cl_2, 17 h; d) Z-Phe-OH, HBTU, DIPEA, DMF; e) 1. Fmoc-Glu(OAll)-OH, HBTU, DIPEA, DMF, 2. 20% piperidine/DMF; f) $Pd(PPh_3)_4$, CH_2Cl_2/NMM/HOAc (8:2:1), 4 h, Ar; g) HATU, DIPEA, HMC or HC or AMC, DMF, 5 h; h) HFIP/CH_2Cl_2 (1:4), 3×10 min.

the uronium-based coupling agent (1-[bis(dimethylamino)-methylene]-1*H*-1,2,3-triazolo[4,5-b]pyridinium 3-oxid hexafluorophosphate (HATU) and *N*,*N*-diisopropylethylamine (DIPEA) as base gave complete conversion of the carboxylic acids into the corresponding coumarinyl esters (Discussion S3).[18] Subsequent release of the acyl donors from the resin was achieved under mild conditions by treatment with a 1:4 mixture of hexafluoroisopropanol (HFIP) and dichloromethane.[19] In this context, the use of HFIP instead of trifluoroacetic acid (TFA) ensures the integrity of the coumarinyl esters, because they are potentially susceptible to acid-mediated hydrolysis. All compounds were obtained in sufficient yields (26–36%) and high purities after purification by preparative RP-HPLC (see Discussion S4 for details of the experimental procedures).

The established modular solid-phase synthesis approach allows facile access to a variety of peptidic coumarinyl esters in small amounts. In an alternative approach, Chung et al. prepared the analogous chromogenic acyl donor Z-Glu(O*p*Np)-Gly-OH in solution by starting from Z-protected glutamic anhydride, which offers the advantage that the final product can be obtained at a larger scale.[20]

The transfer of the conditions for on-resin esterification to the coupling of AMC to the glutamate side chain carboxylic acid group of resin-linked Z-Glu-Gly-OH yielded only minor amounts of the desired coumarinyl amide **5c** (yield 3%, Discussion S5) along with different side products. This might be the result of the less nucleophilic character of the aromatic amine AMC under these conditions, relative to the aromatic alcohols HMC and HC. To increase the yield for this amidation, different coupling procedures were tested with limited success (for details and further information see Discussion S5). However, the amounts of **5c** obtained by the various synthetic methods were sufficient for initial investigations into its behaviour towards TGase 2.

To determine the solubilities of the new glutamate-derived fluorogenic acyl donors **3**-**6**, the compounds were investigated with regard to the rates of their spontaneous reactions at pH 8.0 in the presence of 5% DMSO, as previously done for **2a** and **2b**. The resulting plots showed linearity up to concentrations of 250 μM (see Figure 1 for the acyl donor **5b** and Figure S4); this highlights that the presence of the carboxylic acid group significantly increases the solubility relative to the γ-Abu derivatives. Whereas linearity predominates over the entire concentration range for compound **4**, a slight bend between 100 and 200 μM is visible for compound **5b**; this indicates a diminished solubility at 200 and 250 μM. This behaviour can also be observed for the other glutamate-derived acyl donors **3**, **5a**, **6a** and **6b** (Figure S4). Nevertheless, enzyme-kinetics investigations up to substrate concentrations of 200–250 μM should also be possible for these acyl donors, because they still exhibit sufficient solubility in this concentration range. Notably, none of the glutamate-derived acyl donors forms any visible precipitate up to concentrations as high as 500 μM. Furthermore, as indicated in Figure S4, the extents of the spontaneous reactions vary within the different acyl donors. To quantify these characteristics, pseudo-first-order rate constants (k_{obs}) for the spontaneous reactions, summarised in Table 2, were determined for all ester-based acyl donors.

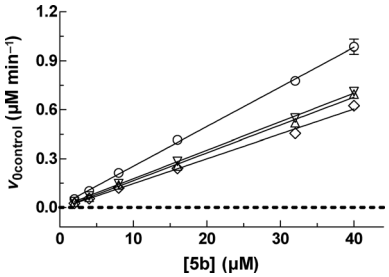

Figure 1. Spontaneous reactions of the fluorogenic acyl donor **5b**. Plots of $v_{0control} = f([\mathbf{5b}])$ at pH 8.0 and 30 °C in the presence of 5% DMSO and 500 μM DTT (○), 500 μM TCEP (△), no additive (▽) and 400 μM aminoacetonitrile (◇). Analysis by linear regression (——) gave rate constants k_{obs} of $(24.3 \pm 1.1) \times 10^{-3}$ min^{-1} (DTT), $(17.1 \pm 0.4) \times 10^{-3}$ min^{-1} (TCEP), $(17.5 \pm 0.2) \times 10^{-3}$ min^{-1} (no additive) and $(15.3 \pm 0.2) \times 10^{-3}$ min^{-1} (aminoacetonitrile). Data shown are mean values ± SEMs of two separate experiments, each performed in duplicate. When not apparent, error bars are smaller than the symbols.

Table 2. Pseudo-first-order rate constants (k_{obs}) for the spontaneous reactions of the different acyl donors at pH 8.0 and 30 °C.

	k_{obs} ($\times 10^{-3}$ min^{-1})		
Acyl donor	DTT	TCEP	k_{obs}(TCEP)/k_{obs}(DTT)
2a	15.8 (0.6)	2.11 (0.05)	0.13
2b	14.3 (0.5)	1.86 (0.08)	0.13
3	–	4.60 (0.36)	–
4	12.2 (0.2)	4.75 (0.13)	0.39
5a	25.1 (2.8)	16.9 (0.6)	0.67
5b	24.3 (1.1)	17.1 (0.3)	0.70
6a	29.2 (4.0)	18.1 (0.5)	0.62
6b	32.7 (1.1)	25.3 (0.4)	0.77

Data shown are mean values ± standard errors of the means (± SEMs) of two to three separate experiments, each performed in duplicate. The corresponding plots of $v_{0control} = f$([acyl donor]) are given in the Supporting Information (Figure S5).

Because the assay of TGase 2 requires the presence of an antioxidant to prevent oxidation of the active-site cysteine residue, both DTT and tris(2-carboxyethyl)phosphine (TCEP) were employed for investigations into the spontaneous reactivity of the compounds at a concentration of 500 μM. In the presence of TCEP, the obtained k_{obs} values reveal distinct spontaneous reactions for all compounds; these seem to depend on the kind of the peptidic scaffold and thus allow for a classification into three groups. The γ-aminobutyroyl derivatives **2a** and **2b** display the lowest k_{obs} values. Compounds **3** and **4**, each bearing a free carboxylic acid group directly on the glutamate residue, exhibited pseudo-first-order rate constants approximately twice those of their descarboxy analogues. Interestingly, C-terminal extension with glycine resulted in k_{obs} values that were increased by a factor of approximately four, as observed for the acyl donors **5a**, **5b**, **6a** and **6b**.

These results suggest that the carboxylate group might act as an intramolecular general base to facilitate the nucleophilic attack of water on the coumarinyl ester bond. General intramo-

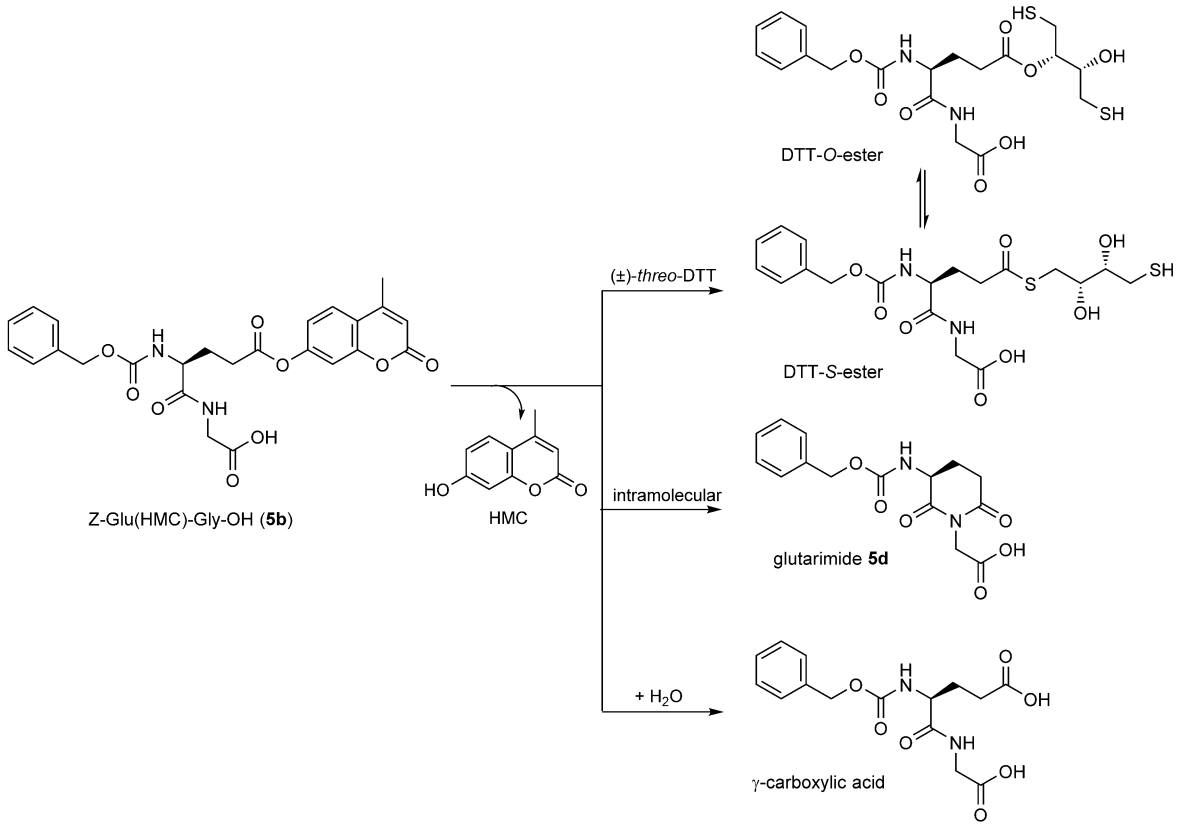

Scheme 4. Structures of identified products from spontaneous reactions of **5 b**.

lecular base catalysis is obviously more effective for the glycine derivatives, because a spatial orientation of the glycine carboxylic acid group in proximity to the coumarinyl ester bond is probably sterically less strained than that of the glutamate carboxylic acid group (Figure S5).

Monitoring of the spontaneous reactions in the presence of DTT resulted in k_{obs} values up to 1.6 times greater than those determined in the presence of TCEP for the glutamate-derived acyl donors and up to 7.6 times greater for the γ-Abu derivatives **2 a** and **2 b** (Figure 1 and Table 2). Because of the nucleophilic character of its two thiol groups, DTT might contribute to the spontaneous reaction of the ester substrates. This pathway of spontaneous substrate disintegration is very likely to occur; reactions between activated aryl esters and thiols to afford thioesters having previously been reported.[21] In general, thioesters are distinctly more stable towards hydrolysis than the corresponding *O*-esters,[22] so thiolysis of the coumarinyl-ester-based substrates by DTT should be considered an independent pathway for spontaneous reaction. To validate this assumption and to identify the thiolysis products, compound **5 b** was exposed to a tenfold excess of DTT in acetonitrile as solvent in the presence of one equivalent of triethylamine. After 5 h at room temperature, analysis of the reaction mixture by RP-HPLC indicated the formation of three major components in addition to remaining reactant, the released 4-methylumbelliferone and the corresponding γ-carboxylic acid. These were identified as DTT-thioester, DTT-*O*-ester and glutarimide **5 d** (Scheme 4 and Figures S6 and S7). The **5 b**-derived DTT-thioester and *O*-ester, as well as the corresponding glutarimide **5 d**, were also detectable under the assay conditions (pH 8.0, 500 μM DTT) in the absence of TGase 2 (Figure S8). Notably, the rate of spontaneous reaction in the absence of DTT and TCEP is nearly identical to that observed in the presence of TCEP, which illustrates that the presence of TCEP does not contribute to the spontaneous disintegration of the acyl donors (Figure 1). Glutarimide formation from **5 b** under assay conditions was unexpected; however, this cyclisation does not substantially contribute to the spontaneous disintegration of **5 b** (Figure S8).

Another type of spontaneous reaction that can occur during investigations into TGase 2-catalysed aminolysis is spontaneous aminolysis. However, as shown for compound **5 b**, for example, in Figure 1, no increased rate constant for spontaneous disintegration was observed in the presence of aminoacetonitrile and concomitant absence of any reducing agent.

In conclusion, because all coumarinyl esters exhibit distinct rates of spontaneous reactions at pH 8.0, these nonenzymatic conversions must be considered for analyses of TGase 2-mediated hydrolyses and aminolyses to ensure correct data evaluation. For this purpose, control measurements in the absence of TGase 2 were carried out for the characterisation of all substrates to determine the proportions of the enzyme-catalysed reactions.

Kinetic analysis of TGase 2-catalysed conversions of the glutamate-derived acyl donors

TGase 2-catalysed hydrolyses: Prior to the characterisation of the different acyl donors, fluorescence coefficients for the fluorophores HC and HMC were determined. As can be seen in Figure S17, sufficient linearity between the concentration of fluorophore and the associated fluorescence signal is predominant up to a concentration of 20 μM. Example kinetic runs for the enzymatic hydrolysis and the spontaneous reaction at pH 8.0 are depicted for compound **5b** in Figure 2. The enzymatic measurements for compound **5b** generated nonlinear progress curves over 900 s; these have also been observed for the other compounds, including the γ-aminobutyric acid derivatives **2a** and **2b**. To ensure that inactivation of TGase 2 does not occur due to protein instability under the experimental conditions (which could also account for nonlinear progress curves), the Selwyn test was performed with acyl donor **5b**.[23] The results clearly indicate the absence of enzyme inactivation over the entire measurement period of 900 s: plots of RFU = *f*([E]*t) are almost congruent for three different enzyme concentrations (Figure S9). Therefore, nonlinear progress curves result from rapid enzymatic conversion of the acyl donors, which gradually leads to substrate depletion for TGase 2. Typically, this effect can be simply reduced by using a lower enzyme concentration, as demonstrated by the Selwyn test, which was performed at 1, 2 and 3 μg mL^{-1} of TGase 2. However, with the reduced amount of enzyme the relative proportion of the spontaneous reaction increases (Figure S10). Despite the fact that the portion of the enzymatic rate even at the lowest enzyme concentration is greater than that of the spontaneous rate (over the applied range of substrate concentration), a TGase 2 concentration of 3 μg mL^{-1} provides the best compromise between signal/background ratio and speed of enzymatic reaction. If the concentration of the released fluorophore exceeds 20 μM during the enzymatic conversion of the acyl donor, fluorescence quenching might contribute to the bend of the curves. Hence, progress curves for the enzymatic hydrolyses were analysed over the first 300 s by nonlinear regression with use of Equation (1),[24] which maintained the limits for the fluorescence coefficient discussed above.

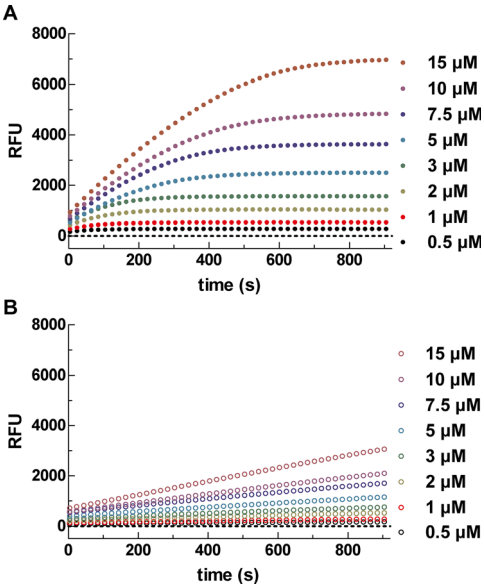

Figure 2. Progress curves for A) TGase 2-catalysed hydrolysis, and B) spontaneous reaction of acyl donor **5b**. Conditions: pH 8.0, 30 °C, 5% DMSO, 500 μM DTT, 3 μg mL^{-1} gpTGase 2.

Michaelis–Menten plots for the enzymatic hydrolysis of compound **5b** by gpTGase 2 and by hTGase 2 at pH 8.0 are depicted in Figure 3 (for the other compounds, see Figures S11 and S12). The obtained kinetic parameters for all compounds are summarised in Table 1. The ratio k_{cat}/K_m, which we decided to denote as performance constant according to Koshland's suggestion, can be regarded as the most appropriate parameter for comparing the synthesised fluorogenic acyl donors with regard to their TGase 2-catalysed conversion.[25] Relative to **2b**, changing γ-Abu to glutamate resulted in a significantly decreased k_{cat}/K_m value for compound **4** (456 000 M^{-1} s^{-1} and 16 400 M^{-1} s^{-1} for **2b** and **4**, respectively), mainly due to an increase in K_m. This result indicates a detrimental effect on the affinity towards gpTGase 2 when the carboxylic acid group is directly attached at the glutamate residue; this is in agreement with previous results observed with substrates that contain glutamine[26] or with inhibitors based on reactive glutamine analogues.[27] Therefore, a shift of the carboxylic acid group further away from the reaction centre might be beneficial for the recognition by gpTGase 2.

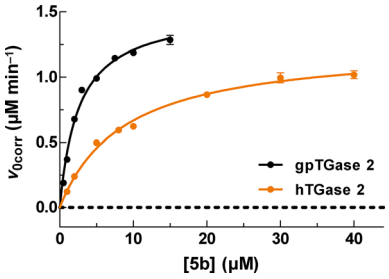

Figure 3. gpTGase 2- and hTGase 2-catalysed hydrolysis of the acyl donor **5b** at pH 8.0. Plots of $v_{0corr} = f$([acyl donor]) with the nonlinear regressions (——) with use of Equation (4) (Michaelis–Menten equation, Experimental Section). Data shown are mean values ± SEMs of three separate experiments, each performed in duplicate. When not apparent, error bars are smaller than the symbols. Conditions: pH 8.0, 30 °C, 5% DMSO, 500 μM DTT (for gpTGase 2) or 500 μM TCEP (for hTGase 2), 3 μg mL^{-1} of either gpTGase 2 or hTGase 2.

Indeed, compound **6b**, with Z-Phe-Glu-Gly-OH as peptidic scaffold, shows a performance constant more than one order of magnitude higher (k_{cat}/K_m = 207 000 M^{-1} s^{-1}) than that of **4**. In order to define the minimal peptidic motif for efficient TGase 2-mediated conversion, N-terminal deletion of the Phe residue was envisaged. For this purpose, we synthesised compounds **3** and **5b**, derived from Z-Glu-OH and Z-Glu-Gly-OH, respectively. From the kinetic data, it can be concluded that the presence of the N-terminal phenylalanine residue does not

seem to be crucial for efficient conversion by gpTGase 2 because the performance constants even increase upon its deletion (compare **3** and **4** as well as **5b** and **6b**). Again, the presence of a C-terminal glycine residue positively influenced the recognition by gpTGase 2 (k_{cat}/K_m values of 41300 and 300000 $M^{-1}s^{-1}$ for **3** and **5b**, respectively). In order to evaluate the influence of the fluorophore on the substrate properties, HC analogues of the best HMC-bearing substrates **5b** and **6b** were synthesised. Surprisingly, whereas **5a** displays almost unaltered kinetic parameters, characterisation of tripeptide **6a** revealed a considerably lower performance constant in comparison with its methyl-substituted counterpart **6b**. This result suggests that the methyl group in the 4-position of the coumarin system might be beneficial but in detail its influence seems to depend on the peptidic scaffold. Finally, comparison of **5b** ($k_{cat}/K_m = 300000\ M^{-1}s^{-1}$) with acyl donors reported in the literature showed that the compound displays not only the most favourable substrate properties of all readily soluble fluorogenic substrates investigated in this study, but also belongs to the kinetically most favourable acyl donor substrates for gpTGase 2 described so far.[11] However, it should be pointed out that, out of all investigated fluorogenic acyl donors, compound **2b** ($k_{cat}/K_m = 456000\ M^{-1}s^{-1}$) clearly exhibits the best kinetic properties, even though it is the least soluble compound of the series.

In accordance with this result, the corresponding non-fluorescent substrate Z-Gln-Gly-OH exhibits favourable kinetic parameters towards gpTGase 2[26] and a microbial transglutaminase.[28] In addition to the evaluation of the acyl donors towards gpTGase 2, compounds **5a**, **5b** and **6b**, which display favourable substrate properties towards that enzyme, were also characterised with regard to their hydrolysis catalysed by human TGase 2. The two orthologues share 83% sequence identity, which in turn makes TGase 2 from guinea pig liver a cost-efficient model for the human enzyme (Figure S13).[29] Notably, all three compounds are also suitable substrates for hTGase 2, even though performance constants are diminished relative to those of the guinea pig enzyme (Table 1).

Their K_m values are four to five times higher than for the gpTGase 2. Trends are similar to those for gpTGase 2, and compound **5b** turned out to be the acyl donor with the most favourable substrate properties towards the human enzyme ($k_{cat}/K_m = 78900\ M^{-1}s^{-1}$). A Michaelis constant similar to that of **5b** has been reported for the chromogenic analogue Z-Glu(O*p*Np)-Gly-OH towards hTGase 2, with a similar tendency being found on comparison with the guinea pig enzyme.[31]

An experimental setup with 96-well plates was used to record spontaneous and enzymatic hydrolyses simultaneously, so there is a time delay between the start of the reaction and the data acquisition. In consequence, those substrate concentrations pipetted at earlier time points might be lower than intended at the start of the measurement. Although it was attempted to minimise this problem by pipetting in the right order of substrate concentrations—that is, from low to high—it cannot be completely avoided. The resulting variation of the substrate concentrations is not considered by the classical regression analysis but can be quantified by analysis with numerical integration. Furthermore, application of this method was envisaged in order to test whether or not separate recording of spontaneous and enzymatic reactions is of sufficient accuracy to allow calculation of the kinetic parameters for the enzyme-catalysed reactions. For this purpose, the differential equations for the time dependence of [E], [SL], [ESL] and [P] of the classical two-step Michaelis–Menten model extended by the pathway for spontaneous reaction of the acyl donor substrates were formulated (Scheme 5) and implemented in the

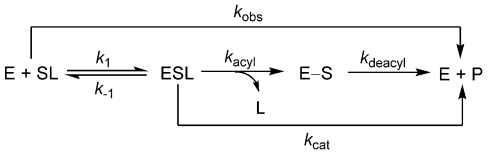

Scheme 5. Kinetic model for substrate hydrolysis by TGase 2 and the corresponding differential rate laws derived from it. The kinetic model was prepared according to ref. [32]. For all calculations, rate constants k_{acyl} and k_{deacyl} were combined to rate constant k_{cat} according to the equation: $k_{cat} = k_{acyl} \times k_{deacyl}/(k_{acyl} + k_{deacyl})$. Abbreviations used in the scheme. E: enzyme. SL: substrate (fluorogenic acyl donor). ESL: initial enzyme·substrate complex. L: coumarin derivative. E–S: acylated enzyme intermediate. P: product.

freely available statistical software R (www.r-project.org/; see the Experimental Section for further details). The kinetic parameters K_m and k_{cat} obtained from nonlinear regressions were then used as initial values for numerical integration of the corresponding progress curves (same data sets as for analysis by nonlinear regression) over the first 300 s. Global fits to the data from one example experiment for compound **5b** are shown in Figure 4. As is obvious, a global fit to the experimental data provided the best-fit traces of sufficient quality for all concen-

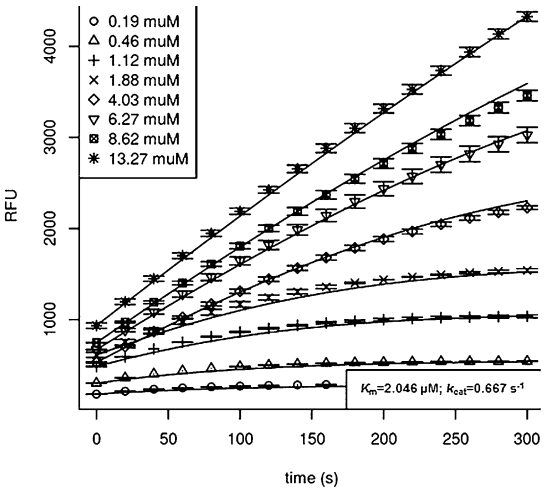

Figure 4. Global fit of progress curves for gpTGase 2-catalysed hydrolysis of acyl donor **5b** at pH 8.0. Concentrations of **5b** at the start of the reaction were 0.5 (○), 1 (△), 2 (+), 3 (×), 5 (◇), 7.5 (▽), 10 (■) and 15 µM (*). Data shown [mean ± standard deviation (±SD)] are from one experiment that was performed in duplicate. The calculated concentrations at the time point of data acquisition are given in the box in the top-left corner. Fitted values for K_m and k_{cat} are given in the box in the bottom-right corner; values calculated from three independent experiments can be found in Table 1. Conditions: pH 8.0, 30 °C, 5% DMSO, 500 µM DTT, 3 µg mL^{-1} gpTGase 2.

trations. In this context, deviations of fit traces from experimental data are a common problem of analysis by global fitting because "it is not permissive to even small deviations from ideal progress curves, that is, data should not contain errors and should perfectly adhere to the model".[33] With regard to the calculation of mean values and errors for K_m and k_{cat}, the experiments for each acyl donor were separately analysed by global fitting followed by statistical analysis of the obtained fitted parameters (Table 1). Notably, both methods for data analysis gave reasonably comparable results for the values of K_m and k_{cat}. Thus, the approach used to determine the proportion of enzyme-catalysed reaction within the regression analysis by simple subtraction of the rates for spontaneous reaction from those of the overall reaction seems to be of sufficient accuracy. However, the systematic deviation to lower values for the parameters derived from numerical integration in relation to those obtained by nonlinear regression might occur due to the corrected substrate concentrations, which highlights the advantage of the former method.

Kinetic behaviour of coumarinyl amide **5c**: The distinct spontaneous reaction of the coumarinyl esters requires careful handling of these compounds and more complex data evaluation. Therefore, a substrate analogue with substrate properties similar to those of the coumarinyl esters but that is devoid of spontaneous disintegration would be advantageous. A promising way to obtain such a substrate seemed to be the exchange of the ester bond between the fluorophore and the peptidic scaffold for an amide bond. From the investigations done in this study with regard to the substrate properties of different peptidic scaffolds, the dipeptide Z-Glu-Gly-OH seemed to be most suitable for performing such a substitution. Therefore, compound **5c**, bearing AMC attached at the carboxylic acid group of the glutamate side chain, was synthesised.

Indeed, no spontaneous release of AMC was observed in the absence of TGase 2 (Discussion S6). Surprisingly, though, initial investigations of **5c** with regard to its enzymatic hydrolysis and aminolysis also revealed no TGase 2-mediated release of AMC (Discussion S6), and the same was also observed for the γ-Abu-derived coumarinyl amide **2c**, as mentioned above. This was not expected for the coumarinyl amides, because TGase 2 is actually specialised in the interconversion of amide bonds. Moreover, aryl amides should be easier to cleave than aliphatic amides from a purely electronic point of view, due to the less pronounced double bond character of an amide bond adjacent to an aromatic ring system. This situation can also result in faster reactions catalysed by enzymes involving acyl-enzyme intermediates such as the serine protease trypsin, for which nitroanilide substrates exhibited greater performance constants than the corresponding primary amides.[34] However, results comparable to those reported here were also obtained from studies on chromogenic and fluorogenic acyl donor substrates for factor XIIIa. Rapid cleavage of the aryl amide bond by factor XIIIa to release *p*-nitroaniline was observed, whereas the conversion of the corresponding AMC derivatives was considerably slower. In contrast, the conversion of both aryl-amide-based substrates by TGase 2 was negligible.[35]

To obtain further information on the kinetic behaviour of compound **5c**, the gpTGase 2-catalysed hydrolysis of coumarinyl ester **5b** in the presence of increasing concentrations of **5c** was studied (Discussion S6). Judged from these results, **5c** has an inhibitory effect on the enzymatic hydrolysis of **5b**. A detailed kinetic analysis of the recorded data can be found in Discussion S6. In summary, the obtained results indicate that the coumarinyl amide seems most likely to act as a linear ($\beta = 0$) mixed, predominantly specific ($1 < \alpha < \infty$) inhibitor according to the systematic classification of enzyme-modifier interactions suggested by Baici[1].[36] In view of the high structural similarity between the coumarinyl ester **5b** and the coumarinyl amide **5c**, the observed pronounced competitive component for inhibition of gpTGase 2 by **5c** is comprehensible. On the other hand, binding of **5c** to sites distinct from the active site also appears to be reasonable if one considers the multidomain structure of the TGase 2 protein, which is known to harbour several binding sites for various ligands apart from the catalytic centre. As a representative example, Yi et al. recently reported on an acylidenoxindole derivative that also exhibits inhibitory potency of noncompetitive character on the transamidase activity.[37]

TGase 2-catalysed aminolysis: Transglutaminases are specialised in the catalysis of transamidation reactions with primary-amine-derived acyl acceptors, so the kinetics of TGase 2-catalysed aminolysis of the glutamate-derived acyl donors—with aminoacetonitrile as amine substrate—were investigated in addition to hydrolysis.

The corresponding kinetic data are shown in Table 3, with the parameters K_m and k_{cat} being of apparent character (see Discussion S7 for detailed explanation). Nevertheless, K_m^{app} and k_{cat}^{app} can be used to evaluate the different substrates because they were determined under identical conditions at an aminoacetonitrile concentration of 400 μM, thus guaranteeing excess over the corresponding acyl donor. However, the calculated ratios of k_{cat}^{app} to K_m^{app} represent the true performance constants for aminolysis, because V_{max}/K_m is independent of the concentration of either substrate, if the enzyme-catalysed reaction adheres to a ping-pong mechanism,[38] which is the case for TGase 2.[39,32b] The dependence of the kinetic parameters K_m^{app} and k_{cat}^{app} on substrate structure followed the trends observed for hydrolysis; however, the values are considerably greater (Table 3 and Figure 5). This result is reasonable because the deacylation step with aminoacetonitrile as acyl acceptor substrate proceeds considerably more rapidly than in water.[20b] Because the Michaelis constant is the ratio of the sum of the rate constants that describe the steps of disintegration of the Michaelis complex ($k_{-1} + k_{cat}$) divided by the second-order rate constant for the association of free enzyme and substrate (k_1), the values for K_m have to increase as deacylation becomes faster. This relationship results in apparent K_m values up to approximately 100 times higher than the Michaelis constants for hydrolysis. Consequently, the increased single parameters K_m and

[1] *In that system for classification of enzyme–modifier interactions, competitive inhibition is referred to as specific inhibition whereas noncompetitive inhibition is referred to as catalytic inhibition.*

Table 3. Kinetic parameters for the TGase 2-catalysed aminolysis of the acyl donors **3**–**6** at pH 8.0 and 30 °C with aminoacetonitrile (400 μM) as acyl acceptor.

Cpd	Regression analysis			Numerical integration		
	K_m^{app} [μM]	k_{cat}^{app} [s^{-1}]	k_{cat}/K_m [$M^{-1}s^{-1}$]	K_m^{app} [μM]	k_{cat}^{app} [s^{-1}]	k_{cat}/K_m [$M^{-1}s^{-1}$]
	gpTGase 2					
3	148 (52)	6.26 (1.26)	42300	99.5 (13.9)	4.28 (0.17)	43000
4	140 (24)	3.05 (0.39)	21800	135 (19)	2.66 (0.29)	19600
5a	120 (12)	47.1 (3.6)	393000	82.9 (7.6)	34.3 (1.1)	414000
5b	121 (8)	52.7 (1.7)	436000	82.1 (3.6)	35.7 (0.5)	435000
6a*	236	29.7	126000	249 (104)	29.8 (9.5)	120000
6b*	238	70.4	296000	150 (21)	45.6 (4.2)	304000
	hTGase 2					
5b*	252	22.7	90100	171 (51)	16.7 (4.6)	97800

For details on calculation of the kinetic parameters see the Experimental Section. Data shown are mean values (±SEMs) of three separate experiments, each performed in duplicate. Active concentrations of TGase 2 from guinea pig liver (E_T = 3.16 nM for **5**–**6** and 21.0 nM for **3** and **4**) and from human TGase 2 (E_T = 3.08 nM) were calculated from Zedira's activity data or determined by active site titration as recently described,[30] respectively. * Data obtained by the method of Cornish-Bowden and Eisenthal.[40]

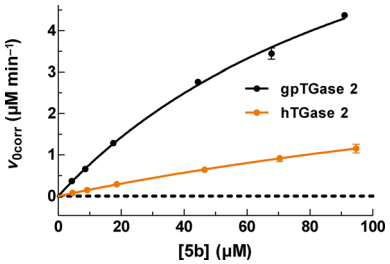

Figure 5. gpTGase 2- and hTGase 2-catalysed aminolysis of acyl donor **5b** at pH 8.0. Plots of $v_{0corr} = f([\mathbf{5b}])$ with nonlinear regressions (——) with use of the Michaelis–Menten equation [Eq. (4), Experimental Section]. Data shown are mean values ±SEMs of three separate experiments, each performed in duplicate. When not apparent, error bars are smaller than the symbols. Conditions: pH 8.0, 30 °C, 5% DMSO, 500 μM TCEP, 400 μM aminoacetonitrile, 0.3 μg mL^{-1} of either gpTGase 2 or hTGase 2.

k_{cat} compensate each other when the performance constants are calculated, with the latter ones being of similar value to those of the hydrolysis reaction. As in the case of hydrolysis, **5b** was revealed to be the most efficient substrate, with a performance constant of 436000 $M^{-1}s^{-1}$ towards TGase 2 from guinea pig, whereas its reaction with aminoacetonitrile catalysed by the human enzyme was much slower (k_{cat}/K_m = 90100 $M^{-1}s^{-1}$).

Representatively for compound **5b**, additional investigations that allowed for estimation of its true kinetic parameters k_{cat} and K_m were performed (Discussion S7). Because of the high values of K_m^{app}, measurements at higher acyl donor concentrations were necessary, and this in turn resulted in higher rates of spontaneous reactions. For regression analysis, the initial substrate concentrations were therefore corrected to allow for the time delay between preparation of the reaction mixture and the start of reaction by addition of the enzyme. Furthermore, fitting the Michaelis–Menten equation to the experimental data yielded unreliable results in the cases of compounds **6a** and **6b**, as well as for **5b**, in the presence of hTGase 2, due to the high K_m^{app} values and limitations in substrate concentration. For this reason, evaluation of these data sets was performed by the method of Cornish-Bowden and Eisenthal (Figures S14 and S15).[41,40] The results of data analysis by numerical integration are in good agreement with those obtained by regression analysis (Table 3).

Exceptions can be observed for the K_m^{app} values of **6b** in the presence of gpTGase 2 and of **5b** in that of the human enzyme obtained from the different methods of data analysis. These discrepancies might result from the mentioned problem that in those cases substrate concentrations were restricted to values $< K_m^{app}$. In this context, it might seem that the improved solubility of the glutamate-derived acyl donors in relation to the γ-Abu derivatives is of minor importance because substrate concentrations $< K_m^{app}$ could also be investigated for the latter compounds. However, the observed increase in K_m upon changing the acyl acceptor from water to aminoacetonitrile, which was also demonstrated for compound **2a** by Gillet et al.,[12] implicates that substrate concentrations for **2a** and **2b** would be restricted to even lower values in relation to K_m^{app}. Although we refrained from attempts to characterise **2a** and **2b** with regard to their enzymatic aminolyses, it can be concluded that the increased solubility of the glutamate-derived acyl donors might indeed be beneficial, because a broader concentration range is available for these substrates.

To confirm the occurrence of TGase 2-catalysed transamidation in the presence of competing spontaneous reaction pathways, the assay mixture containing **5b** and aminoacetonitrile was analysed by RP-HPLC and ESI-MS, which confirmed the formation of the expected corresponding cyanomethyl amide (Figure S16).

Application of acyl donor 5b for the kinetic characterisation of amine substrates and inhibitors

Characterisation of amine substrates: One motivation behind this study was to establish an activity assay for TGase 2 that allows kinetic evaluation both of amine-based acyl acceptor substrates and of irreversible inhibitors of this enzyme. After identifying fluorogenic acyl donor substrates with suitable properties, we therefore aimed to establish their applicability for that purpose. Because **5b** exhibited the best substrate

properties of the studied analogues, the following investigations were performed with this acyl donor substrate. *N*-(Biotinyl)cadaverine is often applied as amine substrate to determine the activity of TGase 2,[42] so this compound was selected in addition to aminoacetonitrile in order to verify the applicability of the new fluorogenic acyl donors for the kinetic characterisation of primary amines as acyl acceptors (for synthesis see Discussion S8).

The two primary amines were evaluated with regard to their kinetic parameters K_m and k_{cat}, which were determined at a constant concentration of **5b** (100 μM). This concentration of the acyl donor substrate is not sufficient to fulfil the condition $K_m(\mathbf{5b}) \ll [\mathbf{5b}]$, neither for the guinea pig nor for the human TGase 2, so the parameters K_m and k_{cat} are of apparent character and therefore denoted as K_m^{app} and k_{cat}^{app}. The Michaelis–Menten plots are shown in Figure 6, and the calculated parameters are summarised in Table 4.

For aminoacetonitrile, values for K_m^{app} and k_{cat}^{app} of 37 μM and 27 s^{-1}, respectively, were determined with the guinea pig enzyme. With human TGase 2, the K_m^{app} of aminoacetonitrile was slightly lower, whereas its k_{cat}^{app} value decreased to a larger extent, thus resulting in a somewhat reduced performance constant. To gain insights into the true Michaelis constant of aminoacetonitrile, K_m^{app} values were determined at four different concentrations of the fluorogenic acyl donor **5b**, which concomitantly provided insight into the true K_m value of **5b**. The detailed analysis of these kinetic data along with the associated discussion is given in Discussion S7.

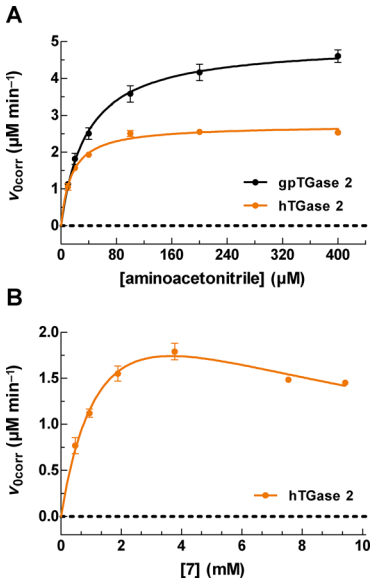

Figure 6. gpTGase 2- and hTGase 2-catalysed incorporation of different amines into compound **5b**. Plots of $v_{0corr} = f([amine])$ with nonlinear regressions (——) with use of **A**) Equation (4) (Michaelis–Menten equation, Experimental Section) for aminoacetonitrile, and **B**) Equation (5) (substrate inhibition, Experimental Section) for *N*-(biotinyl)cadaverine (**7**). Data shown for aminoacetonitrile are mean values ± SEMs of three separate experiments, each performed in duplicate. Data shown for *N*-(biotinyl)cadaverine (**7**) are mean value ± SD of one experiment, performed in duplicate. When not apparent, error bars are smaller than the symbols. Conditions: pH 8.0, 30 °C, 5% DMSO, 100 μM acyl donor **5b**, 500 μM TCEP, 0.3 μg mL^{-1} gpTGase 2 or 0.6 μg mL^{-1} hTGase 2.

Table 4. Kinetic parameters of different amines as acyl acceptors for gpTGase 2 and hTGase 2 at pH 8.0 and 30 °C with compound **5b** (100 μM) as acyl donor.

Amine	K_m^{app} [mM]	k_{cat}^{app} [s^{-1}]	k_{cat}/K_m [$M^{-1}s^{-1}$]
	gpTGase 2		
aminoacetonitrile	0.037 (0.002)	27.0 (1.8)	730000
	hTGase 2		
aminoacetonitrile	0.015 (0.001)	7.39 (0.15)	493000
N-(biotinyl)cadaverine (**7**)*	1.67	9.02	5400

For details of the calculation of the kinetic parameters see the Experimental Section. Data shown are mean values (± SEMs) either of one (compound **7**) or of three (aminoacetonitrile) separate experiments, each performed in duplicate. Active concentrations of TGase 2 from guinea pig liver (E_T = 3.16 nM) and human TGase 2 (E_T = 6.16 nM) were calculated from Zedira's activity data or determined by active site titration as recently described,[30] respectively. * K_i = 8.04 mM.

Because *N*-(biotinyl)cadaverine (**7**) has frequently been used as molecular tool to study TGase 2 at the cellular level, the utility of **5b** for the evaluation of amine-based acceptor substrates was demonstrated for this compound with human TGase 2. In contrast to aminoacetonitrile, compound **7** displayed a K_m^{app} value in the millimolar range. This dramatic difference in the K_m^{app} values reflects the differing basicities of aminoacetonitrile and **7**. Whereas the amino group of aminoacetonitrile exhibits a pK_a value of 5.6 for the conjugate ammonium ion, the corresponding value for **7** is in the range of 10–11.[20b] Because the deacylation of acyl-donor-derived TGase 2 thioester intermediates can only be effected by unprotonated amines,[43] the free substrate concentration of **7** is much lower than that of aminoacetonitrile. Furthermore, Brønsted plots for a series of primary amines as acyl acceptor substrates of varying basicity indicated a correlation between the performance constants of TGase 2-catalysed transamidation and their pK_a values.[20b] It should be noted that the k_{cat}^{app} value of **7** with human TGase 2 is in the same range as that of aminoacetonitrile and that its rate versus concentration plot indicates substrate inhibition (Figure 6B). The latter finding is in accordance with the behaviour of the analogous fluorescent acyl acceptor *N*-(dansyl)cadaverine, which displayed substrate inhibition for TGase 2-catalysed transamidation in the cases both of the guinea pig enzyme and of the human one. This phenomenon has been attributed to the formation of an unproductive complex of the acyl acceptor substrate and free TGase 2.[32a] Moreover, substrate inhibition in enzyme-catalysed group-transferring reactions by the substrate that is devoid of the transferred group (in this case the amine substrate) is very common, due to its premature binding to the free enzyme.[44]

Characterisation of irreversible inhibitors: Evaluation of enzyme inhibitors for the purposes of drug discovery projects is often based on kinetic assays. This is particularly valid for inhibitors that interact with enzymes in an irreversible manner. Therefore, we aimed to validate the usefulness of the developed fluorogenic TGase 2 substrates for the characterisation of inhibitors representatively for substrate **5b** with the established irreversible TGase 2 inhibitors iodoacetamide and the

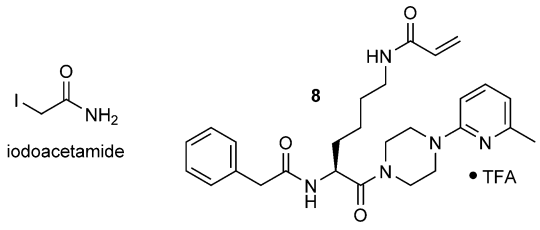

Scheme 6. Structures of iodoacetamide and acrylamide **8**.

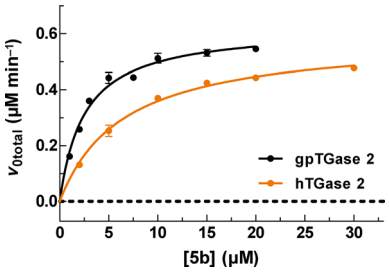

Figure 7. gpTGase 2- and hTGase 2-catalysed hydrolysis of acyl donor **5b** at pH 6.5. Plots of $v_{0total} = f([\mathbf{5b}])$ with the nonlinear regressions (——) by use of Equation (4) (Michaelis–Menten equation, Experimental Section). Data shown are means ± SEMs of three separate experiments, each performed in duplicate. When not apparent, error bars are smaller than the symbols. Conditions: pH 6.5, 30 °C, 5% DMSO, 500 μM TCEP, 3 μg mL^{-1} of either gpTGase 2 or hTGase 2.

recently reported selective N^{ε}-acryloyllysine derivative **8** (Scheme 6).[14]

Inhibition studies with iodoacetamide for the TGase 2-catalysed hydrolysis of **5b** at pH 8.0 were problematic because the product-release progress plots were curved even in the absence of inhibitor, due to substrate depletion (data not shown). To obtain steady-state conditions over a broad time window, neither reducing the amount of enzyme nor increasing the substrate concentration was possible, due to the susceptibility of **5b** to spontaneous hydrolysis. Therefore, the conversion of **5b** was decelerated by reducing the pH from 8.0 to 6.5; this slowed down the rate of the spontaneous reaction to less than 5%, whereas the enzymatic hydrolysis was reduced to a much lesser extent. These modified conditions resulted in linear progress curves for concentrations of **5b** greater than 20 μM both for gpTGase 2 and for hTGase 2 over a time window of 900 s. This linearity ensures the absence of substrate depletion, which is of crucial importance for the correct kinetic evaluation of time-dependent enzyme inhibition.[45] The fluorescence coefficients of 4-methylumbelliferone and the Michaelis–Menten parameters were determined for pH 6.5 (Figures 7 and S17, Table 5).

With gpTGase 2, the performance constants were reduced to 130000 M^{-1} s^{-1}: that is, to less than half of the value determined at pH 8.0 (Table 1). This is caused by a reduction in k_{cat}, with K_m being unaffected by the change in pH. A similar trend was observed for the human enzyme. Data analysis by numerical integration confirmed these results for the two TGase orthologues.

The reduction of pH in the assay medium enabled analysis of inhibition by iodoacetamide under the formalism of slow-binding inhibition [Eq. (6), Experimental Section].[46] Iodoacetamide has been shown to inactivate TGase 2 irreversibly by alkylation of the active-site thiol Cys277.[47] Irreversible enzyme inactivation usually results in steady-state rates that are equal to zero independent of inhibitor concentration. However, because substrate **5b** continues to react in the presence of completely inactivated enzyme, we use v_s as an open parameter in Equation (6) to take account of the remaining spontaneous reaction after completed enzyme inhibition. Replotting the obtained pseudo-first-order rate constants k_{obs} against the inhibitor concentration and linear regression of the resulting line provided the ratio $k_{obs}/[I]$ as slope. Correction of that value by the factor $1 + [S]/K_m$ gave a value of 29800 M^{-1} s^{-1} for the second-order inactivation constant k_{inact}/K_I towards the guinea pig enzyme, with a similar value being obtained for hTGase 2 (Table 6).[46,48] In contrast to the k_{obs} values, which linearly increased with rising inhibitor concentration, the initial velocities did not systematically vary when the iodoacetamide concentration was increased (Figure S18). This finding indicates a one-step mechanism for inactivation of both guinea pig and human TGase 2 by iodoacetamide and suggests that no stable noncovalent enzyme·inhibitor complex is formed prior to the inactivating alkylation step. This result is in agreement with observations for the inactivation of factor XIIIa by iodoacetate[35a] and can be explained by considering that this small-molecule inhibitor does not provide many contact points for noncovalent interactions.

To characterise a pharmaceutically more relevant inhibitor with the established assay, compound **8** was investigated with

Table 5. Kinetic parameters for the TGase 2-catalysed hydrolyses of the acyl donor **5b** at pH 6.5 and 30 °C.

Cpd	Regression analysis			Numerical integration		
	K_m [μM]	k_{cat} [s^{-1}]	k_{cat}/K_m [M^{-1} s^{-1}]	K_m [μM]	k_{cat} [s^{-1}]	k_{cat}/K_m [M^{-1} s^{-1}]
	gpTGase 2					
5b	2.53 (0.18)	0.33 (0.01)	130000	2.62 (0.20)	0.33 (0.01)	126000
	hTGase 2					
5b	6.60 (1.06)	0.32 (0.02)	48500	5.63 (1.00)	0.31 (0.02)	55100

For details on calculation of the kinetic parameters see the Experimental Section. Data shown are mean values (± SEMs) of three separate experiments, each performed in duplicate. Active concentrations of TGase 2 from guinea pig liver (E_T = 31.6 nM) and human (E_T = 30.8 nM) were calculated from Zedira's activity data or determined by active site titration as recently described,[30] respectively. The k_{obs} value for the spontaneous reaction of **5b** at pH 6.5 and 30 °C in the presence of TCEP was determined to be $(0.70 \pm 0.03) \times 10^{-3}$ min^{-1}.

Table 6. Kinetic parameters for the irreversible TGase 2 inhibitors iodoacetamide and acrylamide **8** at pH 6.5 and 30 °C.

Inhibitor	Regression analysis k_{inact}/K_I [$M^{-1}s^{-1}$]	Numerical integration k_{inact}/K_I [$M^{-1}s^{-1}$]
	gpTGase 2	
iodoacetamide	29800 (1280)	39600 (973)
acrylamide **8**	740 (78)	821 (10)
	hTGase 2	
iodoacetamide	50700 (3510)	44400 (3030)
acrylamide **8***	5110 (68)	5290 (135)

*K_i = 5.73 μM (0.77), K_I = 68.7 μM (24.2), k_{inact} = 0.35 s^{-1} (0.12); for details on the calculation of the kinetic parameters see the Experimental Section. Inhibition experiments on gpTGase 2 and hTGase 2 were performed in the presence of 25 μM (≈10×K_m) and 30 μM (≈4.5×K_m), respectively, of acyl donor **5b**. Data shown are mean values (±SEMs) of two separate experiments, each performed in duplicate.

regard to its interaction with guinea pig and human TGase 2. The N^{ε}-acryloyllysine derivative **8** was prepared by the published procedure with slight modifications;[14] details on its synthesis will be reported in the context of a follow-up study. The results of the kinetic characterisation of **8** are included in Table 6. With the guinea pig enzyme, compound **8** exhibited a second-order inactivation constant of 740 $M^{-1}s^{-1}$. No systematic variation of the initial velocities with increasing inhibitor concentration was discernible; this led to the conclusion that inactivation of gpTGase 2 by **8** follows a one-step mechanism. Notably, the situation is obviously different for the human enzyme (Figure 8). Here, the value for k_{inact}/K_I was approximately seven times higher than that for the guinea pig orthologue,

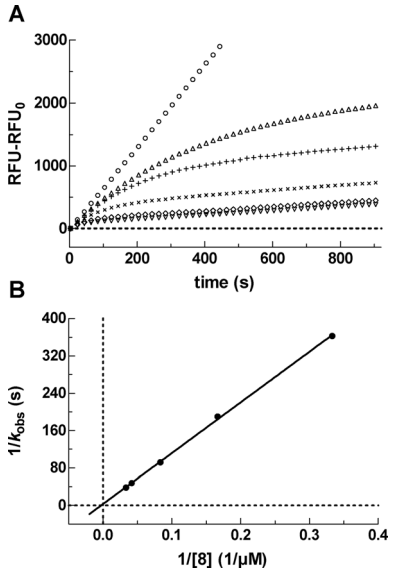

Figure 8. Kinetic characterisation of acrylamide **8** with hTGase 2 and acyl donor **5b**. A) Typical time courses of the hTGase 2-catalysed hydrolysis of **5b** in the presence of different concentrations of acrylamide **8** [0 μM (○), 3 μM (△), 6 μM (+), 12 μM (×), 24 μM (◇) and 30 μM (▽)] in the presence of 30 μM (≈4.5×K_m) of acyl donor **5b**. B) Double reciprocal plot [$1/k_{obs} = f(1/[\mathbf{8}])$] with linear regression to the data for determination of k_{inact}, K_i and k_{inact}/K_I. Conditions: pH 6.5, 30 °C, 5% DMSO, 500 μM TCEP, 3 μg mL^{-1} of hTGase 2.

and the initial velocities (v_i) hyperbolically decreased with increasing inhibitor concentration. This observation indicates the formation of a rapid-equilibrium noncovalent complex between acrylamide **8** and hTGase 2 prior to the inactivation step, for which a dissociation constant (K_i) of 5.73 μM was calculated from the plot of v_i versus [I] (Figure S19). From the double reciprocal plot of $1/k_{obs}$ versus 1/[I] (Figure 8B) it was possible to obtain the isolated value for the first-order inactivation constant k_{inact} (0.35 s^{-1}) describing the transition of the initial noncovalent enzyme·inhibitor complex to the final covalent complex. From this value, K_I was calculated to be 68.7 μM. The meaning of this value is distinctly different from that of K_i because it represents a merely kinetic parameter that signifies the inhibitor concentration at which the inactivation proceeds with half the maximum rate in the absence of substrate.[46]

Usually, irreversible enzyme inhibition results in steady state rates equal to zero, whereas in the present case these rates are different from zero because substrate conversion continues after completed enzyme inactivation, due to spontaneous hydrolysis. To take this factor into account for the kinetic analysis of TGase 2 inhibition, the kinetic parameters were independently determined by numerical integration.[33,23b] For this purpose, differential equations were formulated on the basis illustrated in Scheme 7 and implemented into the statistical soft-

$$E + I \underset{k_{-2}}{\overset{k_2}{\rightleftharpoons}} EI \xrightarrow{k_{inact}} E\text{-}I$$

$$\frac{d[I]}{dt} = -k_2[E]\cdot[I] + k_{-2}[EI]$$

$$\frac{d[EI]}{dt} = -k_{-2}[EI] + k_2[E]\cdot[I] - k_{inact}[E\text{-}I]$$

$$\frac{d[E\text{-}I]}{dt} = k_{inact}[EI]$$

Scheme 7. Kinetic model for the two-step irreversible inhibition of TGase 2 and the associated differential rate laws derived from it. For the case that the ratio $k_{-2}/k_2 = K_i$ is high, the concentration of the initial noncovalent enzyme·inhibitor complex becomes negligible and, in consequence, the two-step mechanism for irreversible inhibition simplifies to a one-step mechanism. Abbreviations used in the scheme. E: enzyme. I: inhibitor. EI: initial enzyme·inhibitor complex. E–I: covalent enzyme·inhibitor complex.

ware R. The series of progress curves in the absence and in the presence of different inhibitor concentrations were globally fitted, and this provided values for k_{inact}/K_I that are essentially similar to those obtained by conventional regression analysis (Table 6).

Thus, it can be concluded that the common analysis using integrated rate equations and subsequent evaluation of the obtained data yields reliable parameters to describe the inhibitory potency. Taken together, the obtained results demonstrate the suitability of the established assay for the kinetic characterisation of TGase 2 inhibitors.

Conclusions

The recently described acyl donor substrate **2a** and compounds derived from it that release fluorescent coumarins upon enzymatic conversion appear to be attractive substrates for the fluorimetric assay of TGase 2. However, both **2a** and its methyl-substituted analogue **2b** proved to be prone to aggregation in aqueous media; this can hamper detailed kinetic investigations depending on the particular conditions and intended application purposes. Therefore, analogues based on small glutamate-containing peptides were synthesised by a solid-phase approach and were demonstrated to be soluble in the assay medium up to concentrations of 250 μM. This remarkably improved water solubility allowed for the extensive kinetic characterisation of the newly designed substrates in terms of their TGase 2-catalysed hydrolysis and aminolysis, both by conventional regression analysis and by numerical integration. In addition, their spontaneous reactivity under assay conditions was studied in detail, and this has revealed a significant contribution of spontaneous thiolysis in the presence of DTT to the overall rate of spontaneous disintegration, amongst other findings. This result suggests that TCEP should be used as antioxidant instead of DTT.

The influence of the fluorogenic leaving group on the kinetic properties was investigated. Substrates **5b** and **6b**, each containing 7-hydroxy-4-methylcoumarin attached to the γ-carboxylic acid group of the Glu residue, showed superior kinetic properties to their unsubstituted counterparts **5a** and **6a**; analogous amides **2c** and **5c**, containing 7-amino-4-methylcoumarin, are not accepted as substrates. Z-Glu(HMC)-Gly-OH (**5b**) exhibited the best substrate properties out of the synthesised compounds, with performance constants of 300 000 and 436 000 $M^{-1}s^{-1}$ determined for the gpTGase 2-catalysed hydrolysis and aminolysis, respectively, at pH 8.0. Therefore, **5b** was selected for representative kinetic characterisation of amine-based acyl-acceptor substrates and irreversible inhibitors. The determination of performance constants at pH 8.0 was demonstrated for aminoacetonitrile and *N*-(biotinyl)cadaverine as representative primary amine substrates on both guinea pig and human TGase 2. Inhibitor characterisation was based on monitoring and analysing the TGase 2-catalysed hydrolysis of **5b** at pH 6.5, which resulted in reliable second-order inactivation constants for iodoacetamide and compound **8** towards both the guinea pig and the human enzyme.

Furthermore, this study confirmed compounds **2a** and **2b** as potentially suitable substrates for fluorimetric activity determination of TGase 2. In view of their reduced susceptibility to spontaneous reaction relative to that of the glutamate-derived analogues introduced here, **2a** and **2b** might be more advantageous for assaying cellular TGase 2 activities.[12]

Taken together, the results of this study show compound **5b** to be a powerful fluorogenic substrate of guinea pig and human TGase 2. Therefore, this compound allows for robust assay methods to identify and to characterise molecules capable of targeting TGase 2 for therapeutic inhibition and molecular imaging, although its susceptibility to spontaneous decay might stimulate further developments directed towards fluorogenic substrates for this important enzyme.

Experimental Section

General: All commercial reagents and solvents were used without further purification unless otherwise specified. Melting points were determined with a Galen III Boetius apparatus from Cambridge Instruments. Nuclear magnetic resonance spectra were recorded with Varian Unity 400 MHz or Agilent Technologies 400 NMR spectrometers. Spectra were processed by using the programme MestreNova (version 6.1.1-6384).[49] NMR chemical shifts were referenced to the residual solvent resonances relative to tetramethylsilane (TMS). Mass spectra (ESI) were obtained with a Micromass Quattro LC or a Waters Xevo TQ-S mass spectrometer, each driven by Mass Lynx software. Elemental analysis was performed with a LECO CHNS-932 apparatus. Determination of the resin loading was performed with a Thermo Scientific Helios α UV/Vis spectrophotometer.

Chromatography: Thin-layer chromatography (TLC) was performed with Merck silica gel F-254 aluminium plates and visualisation under UV (254 nm) and/or by staining with a ninhydrin solution (0.1%, *m/v*) in ethanol. Preparative column chromatography was carried out with Merck silica gel (mesh size 230–400 ASTM) and solvent mixtures as specified for the particular compounds. Analytical and preparative HPLC of compounds **2**–**7** was performed with a Varian Prepstar system equipped with a UV detector (Prostar, Varian) and an automatic fraction collector (Foxy 200). Two Microsorb C18 60-8 columns (Varian Dynamax 250×4.6 mm and 250×21.4 mm) were used as the stationary phases for analytical and preparative HPLC, respectively. A binary gradient system of 0.1% CF_3COOH/water (solvent A) and 0.1% CF_3COOH/CH_3CN (solvent B) at a flow rate of 1 mL min^{-1} or 10 mL min^{-1} served as the eluent. For analytical HPLC, the programme for elution of compounds **2**–**6** was as follows: 0–3 min 90% A, 3–25 min gradient to 90% B, 25–35 min 90% B, 35–36 min gradient back to 90% A, 36–40 min 90% A. For compound **7** the following elution regime was used: 0–5 min 95% A, 5–25 min gradient to 95% B, 25–30 min 95% B, 30–31 min gradient back to 95% A, 31–35 min 95% A. For preparative HPLC, the conditions for the gradient elution of compounds **2**–**6** were as follows: 0–3 min 90% A, 3–25 min gradient to 90% B, 25–30 min 90% B, 30–31 min gradient back to 90% A, 31–35 min 90% A. For compound **7** the following elution regime was used: 0–7 min 90% A, 7–22 min gradient to 80% B, 22–30 min 80% B, 30–31 min gradient back to 90% A, 31–35 min 90% A. HPLC for investigating the spontaneous reactivity of compound **5b** was carried out with a system consisting of a Merck Hitachi L7100 gradient pump combined with a Jasco DG2080 four-line degasser with UV detection with a Merck Hitachi L7450 diode array detector. The system was operated with D-700 HSM software and use of a Merck Hitachi D7000 interface. A Luna C18 5 μm column (Phenomenex, 250×4.6 mm) served as stationary phase. The following elution programme (binary gradient system as detailed above, flow rate 1 mL min^{-1}) was run to separate the components: 0–3 min 80% A, 3–25 min gradient to 70% B, 25–26 min gradient to 95% B, 26–30 min 95% B, 30–35 min gradient back to 80% A, 35–40 min 80% A.

Analytical data for the glutamate-derived fluorogenic acyl donors

*Z-L-Glu(HMC)-OH (**3**)*: The synthesis with use of HMC yielded **3** (67 mg, 30%) as a yellow oil. Because **3** tends to decompose in the

isolated state, this compound should be stored below 0 °C. ^{1}H NMR ([D$_6$]DMSO): δ = 7.81 (d, $^3J_{H,H}$ = 8.7 Hz, 1H; H-5 of coumarin), 7.70 (d, $^3J_{H,H}$ = 8.3 Hz, 1H; NH), 7.39–7.27 (m, 5H; H_{phenyl}), 7.25 (d, $^4J_{H,H}$ = 2.1 Hz, 1H; H-8 of coumarin), 7.17 (dd, $^3J_{H,H}$ = 8.6, $^4J_{H,H}$ = 2.2 Hz, 1H; H-6 of coumarin), 6.39 (d, $^4J_{H,H}$ = 1.1 Hz, 1H; H-3 of coumarin), 5.10–5.01 (m, 2H; CH_2O of Z), 4.15–4.07 (m, 1H; $C_\alpha H$ of Glu), 2.78–2.65 (m, 2H; $C_\gamma H_2$ of Glu), 2.44 (d, $^4J_{H,H}$ = 1.0 Hz, 3H; CH_3), 2.20–2.09 (m, 1H; $C_\beta HH$ of Glu), 2.01–1.89 ppm (m, 1H; $C_\beta HH$ of Glu); ^{13}C NMR ([D$_6$]DMSO): δ = 173.26, 170.75, 159.60, 156.19, 153.49, 152.95, 152.80, 136.92, 128.32, 127.81, 127.72, 126.40, 118.38, 117.53, 113.73, 110.07, 65.51 (CH_2O of Z), 52.84 (C_α of Glu), 30.24, 25.91, 18.17 ppm (CH_3); MS (ESI$^+$): *m/z* calcd for $C_{23}H_{22}NNaO_8$: 462.12 $[M+Na]^+$; found: 462.1; elemental analysis calcd (%) for $C_{23}H_{21}NO_8$: C 62.87, H 4.82, N 3.19; found: C 60.45, H 5.14, N 3.14.

Z-L-Phe-L-Glu(HMC)-OH (**4**): The synthesis with use of HMC yielded **4** (99 mg, 36%) as a white solid. Because **4** tends to decompose in the isolated state, this compound should be stored below 0 °C. ^{1}H NMR ([D$_6$]DMSO): δ = 8.41 (d, ^3J = 8.0 Hz, 1H; NH of Glu), 7.81 (d, ^3J = 8.6 Hz, 1H; H-5 of coumarin), 7.53 (d, ^3J = 8.6 Hz, 1H; NH of Phe), 7.36–7.15 (m, 12H; H_{phenyl}, H-6,8 of coumarin), 6.39 (s, 1H; H-3 of coumarin), 4.95–4.87 (m, 2H; CH_2O of Z), 4.45–4.36 (m, 1H; $C_\alpha H$), 4.36–4.28 (m, 1H; C_α), 3.02 (dd, ^2J = 13.8, ^3J = 3.8 Hz, 1H; $C_\beta HH$ of Phe), 2.81–2.69 (m, 3H; $C_\beta HH$ of Phe, $C_\gamma H_2$ of Glu), 2.44 (s, 3H; CH_3), 2.26–2.14 (m, 1H; $C_\beta HH$ of Glu), 2.00–1.88 ppm (m, 1H; $C_\beta HH$ of Glu); ^{13}C NMR ([D$_6$]DMSO): δ = 172.94, 171.91, 170.78, 159.60, 155.90, 153.50, 152.95, 152.87, 138.08, 136.89, 129.20, 128.21, 128.04, 127.63, 127.42, 126.38, 126.25, 118.41, 117.52, 113.72, 110.11, 65.21 (CH_2O of Z), 56.10, 50.69, 37.26, 29.86, 26.10, 18.17 ppm (CH_3); MS (ESI$^+$): *m/z* calcd for $C_{32}H_{31}N_2O_9$: 587.20 $[M+H]^+$; found: 587.3; elemental analysis calcd (%) for $C_{32}H_{30}N_2O_9$: C 65.52, H 5.15, N 4.78; found: C 63.94, H 5.23, N 4.81.

Z-L-Glu(HC)-Gly-OH (**5a**): The synthesis with use of HC yielded **5a** (34 mg, 35%) as a white solid. Because **5a** tends to decompose in the isolated state, this compound should be stored below 0 °C. ^{1}H NMR ([D$_6$]DMSO): δ = 8.32 (t, ^3J = 5.9 Hz, 1H; NH of Gly), 8.07 (d, ^3J = 9.3 Hz, 1H; H-4 of coumarin), 7.76 (d, ^3J = 8.5 Hz, 1H; H-5 of coumarin), 7.57 (d, ^3J = 8.3 Hz, 1H; NH of Glu), 7.39–7.25 (m, 6H; H_{phenyl}, H-8 of coumarin), 7.15 (dd, ^3J = 8.4, ^4J = 2.2 Hz, 1H; H-6 of coumarin), 6.48 (d, ^3J = 9.6 Hz, 1H; H-3 of coumarin), 5.10–4.98 (m, 2H; CH_2O of Z), 4.22–4.13 (m, 1H; C_α of Glu), 3.83 (dd, ^2J = 17.5, ^3J = 5.9 Hz, 1H; $C_\alpha HH$ of Gly), 3.73 (dd, ^2J = 17.5, ^3J = 5.6 Hz, 1H; $C_\alpha HH$ of Gly), 2.78–2.64 (m, 2H; $C_\gamma H_2$ of Glu), 2.12–2.01 (m, 1H; $C_\beta HH$ of Glu), 1.99–1.86 ppm (m, 1H; $C_\beta HH$ of Glu); ^{13}C NMR ([D$_6$]DMSO): δ = 171.54, 171.07, 170.85, 159.68, 155.94, 154.05, 152.82, 143.81, 136.89, 129.28, 128.30, 127.77, 127.69, 118.61, 116.64, 115.52, 110.08, 65.53 (CH_2O of Z) 53.49, 40.67, 30.01, 27.00 ppm; MS (ESI$^+$): *m/z* calcd for $C_{24}H_{23}N_2O_9$: 483.14 $[M+H]^+$; found: 483.1; elemental analysis calcd (%) for $C_{24}H_{22}N_2O_9$: C 59.75, H 4.60, N 5.81; found: C 58.28, H 4.58, N 5.75.

Z-L-Glu(HMC)-Gly-OH (**5b**): The synthesis with use of HMC yielded **5b** (63 mg, 26%) as a white solid. Because **5b** tends to decompose in the isolated state, this compound should be stored below 0 °C. ^{1}H NMR ([D$_6$]DMSO): δ = 12.58 (s, 1H; COOH), 8.32 (t, ^3J = 5.8 Hz, 1H; NH of Gly), 7.81 (d, ^3J = 8.7 Hz, 1H; H-5 of coumarin), 7.57 (d, ^3J = 8.3 Hz, 1H; NH of Glu), 7.39–7.25 (m, 6H; H_{phenyl}, H-8 of coumarin), 7.18 (dd, ^3J = 8.6, ^4J = 2.2 Hz, 1H; H-6 of coumarin), 6.39 (d, ^4J = 1.2 Hz, 1H; H-3 of coumarin), 5.10–4.99 (m, 2H; CH_2O of Z), 4.22–4.14 (m, 1H; $C_\alpha H$ of Glu), 3.83 (dd, ^2J = 17.5, ^3J = 5.9 Hz, 1H; $C_\alpha HH$ of Gly), 3.73 (dd, ^2J = 17.5, ^3J = 5.7 Hz, 1H; $C_\alpha HH$ of Gly), 2.77–2.65 (m, 2H; $C_\gamma H_2$ of Glu), 2.44 (d, ^4J = 1.1 Hz, 3H; CH_3), 2.13–2.01 (m, 1H; $C_\beta HH$ of Glu), 1.98–1.86 ppm (m, 1H; $C_\beta HH$ of Glu); ^{13}C NMR ([D$_6$]DMSO): δ = 171.56, 171.09, 170.86, 159.60, 155.95, 153.49, 152.95, 152.83, 136.90, 128.31, 127.78, 127.71, 126.37, 118.39, 117.50, 113.72, 110.09, 65.54 (CH_2O of Z), 53.50, 40.68, 30.02, 27.00, 18.17 ppm (CH_3); MS (ESI$^+$): *m/z* calcd for $C_{25}H_{25}N_2O_9$: 497.16 $[M+H]^+$; found: 497.1; elemental analysis calcd (%) for $C_{25}H_{24}N_2O_9$: C 60.48, H 4.87, N 5.64; found: C 59.86, H 4.84, N 5.65.

Z-L-Glu(AMC)-Gly-OH (**5c**): The synthesis with use of AMC yielded **5c** (7.3 mg, 3%) as a white solid. ^{1}H NMR ([D$_6$]DMSO): δ = 10.34 (s, 1H; NH of coumarin), 8.22 (t, ^3J = 5.6 Hz, 1H; NH of Gly), 7.75 (d, ^4J = 1.9 Hz, 1H; H-8 of coumarin), 7.70 (d, ^3J = 8.7 Hz, 1H; H-5 of coumarin), 7.49–7.44 (m, 2H; H-6 of coumarin, NH of Glu), 7.40–7.25 (m, 5H; H_{phenyl}), 6.25 (d, ^4J = 1.0 Hz, 1H; H-3 of coumarin), 5.08–4.95 (m, 2H; CH_2O of Z), 4.14–3.99 (m, 1H; $C_\alpha H$ of Glu), 3.82 (dd, ^2J = 17.4, ^3J = 6.1 Hz, 1H; $C_\alpha HH$ of Gly), 3.73 (dd, ^2J = 17.8, ^3J = 5.5 Hz, 1H; $C_\alpha HH$ of Gly), 2.54–2.43 (m, 2H; $C_\gamma H_2$ of Glu), 2.39 (d, ^4J = 0.7 Hz, 3H; CH_3), 2.11–1.95 (m, 1H; $C_\beta HH$ of Glu), 1.92–1.75 ppm (m, 1H; $C_\beta HH$ of Glu); ^{13}C NMR ([D$_6$]DMSO): δ = 171.84, 171.31, 171.08, 160.01, 159.74, 153.65, 153.09, 142.53, 128.30, 127.76, 127.69, 125.85, 115.04, 114.78, 112.08, 105.42, 65.49 (CH_2O of Z), 27.36, 17.95 ppm (CH_3), 2×C_α and C_γ not visible; MS (ESI$^+$): *m/z* calcd for $C_{25}H_{26}N_3O_8$: 496.17 $[M+H]^+$; found: 496.2.

Z-L-Phe-L-Glu(HC)-Gly-OH (**6a**): The synthesis with use of HC yielded **6a** (44 mg, 35%) as a white solid. Because **6a** tends to decompose in the isolated state, this compound should be stored below 0 °C. ^{1}H NMR ([D$_6$]DMSO): δ = 12.59 (s, 1H; COOH), 8.29–8.22 (m, 2H; NH of Glu and Gly), 8.07 (d, ^3J = 9.5 Hz, 1H; H-4 of coumarin), 7.77 (d, ^3J = 8.5 Hz, 1H; H-5 of coumarin), 7.55 (d, ^3J = 8.5 Hz, 1H; NH of Phe), 7.35–7.10 (m, 12H; H_{phenyl}, H-6,8 of coumarin), 6.48 (d, ^3J = 9.6 Hz, 1H; H-3 of coumarin), 4.96–4.87 (m, 2H; CH_2O of Z), 4.52–4.43 (m, 1H; $C_\alpha H$), 4.38–4.27 (m, 1H; $C_\alpha H$), 3.84 (dd, ^2J = 17.5, ^3J = 6.0 Hz, 1H; $C_\alpha HH$ of Gly), 3.74 (dd, ^2J = 17.5, ^3J = 5.8 Hz, 1H; $C_\alpha HH$ of Gly), 3.04 (dd, ^2J = 13.7, ^3J = 3.8 Hz, 1H; $C_\beta HH$ of Phe), 2.81–2.68 (m, 3H; $C_\beta HH$ of Phe, $C_\gamma H_2$ of Glu), 2.16–2.05 (m, 1H; $C_\beta HH$ of Glu), 1.98–1.86 ppm (m, 1H; $C_\beta HH$ of Glu); ^{13}C NMR ([D$_6$]DMSO): δ = 171.67, 171.12, 171.01, 170.88, 159.68, 155.88, 154.05, 152.89, 143.82, 138.06, 136.88, 129.28, 129.19, 128.20, 128.01, 127.62, 127.42, 126.20, 118.64, 116.64, 115.50, 110.11, 65.23 (CH_2O of Z), 56.14, 51.22, 40.67, 37.25, 29.64, 27.16 ppm; MS (ESI$^+$): *m/z* calcd for $C_{33}H_{32}N_3O_{10}$: 630.21 $[M+H]^+$; found: 630.1; elemental analysis calcd (%) for $C_{33}H_{31}N_3O_{10}$: C 62.95, H 4.96, N 6.67; found: C 61.75, H 5.15, N 7.22.

Z-L-Phe-L-Glu(HMC)-Gly-OH (**6b**): The synthesis with use of HMC yielded **6b** (88 mg, 27%) as a white solid. Because **6b** tends to decompose in the isolated state, this compound should be stored below 0 °C. ^{1}H NMR ([D$_6$]DMSO): δ = 8.29–8.24 (m, 2H; NH of Glu and Gly), 7.81 (d, ^3J = 8.7 Hz, 1H; H-5 of coumarin), 7.55 (d, ^3J = 8.4 Hz, 1H; NH of Phe), 7.34–7.16 (m, 12H; H_{phenyl}, H-6,8 of coumarin), 6.39 (d, ^4J = 1.2 Hz, 1H; H-3 of coumarin), 4.95–4.88 (s, 2H; CH_2O of Z), 4.52–4.44 (m, 1H; $C_\alpha H$), 4.37–4.29 (m, 1H; $C_\alpha H$), 3.84 (dd, ^2J = 17.6, ^3J = 5.9 Hz, 1H; $C_\alpha HH$ of Gly), 3.74 (dd, ^2J = 17.5, ^3J = 5.7 Hz, 1H; $C_\alpha HH$ of Gly), 3.04 (dd, ^2J = 13.8, ^3J = 3.7 Hz, 1H; $C_\beta HH$ of Phe), 2.80–2.68 (m, 3H; $C_\beta HH$ of Phe and $C_\gamma H_2$ of Glu), 2.44 (d, ^4J = 0.9 Hz, 3H; CH_3), 2.17–2.05 (m, 1H; $C_\beta HH$ of Glu), 1.98–1.86 ppm (m, 1H; $C_\beta HH$ of Glu); ^{13}C NMR ([D$_6$]DMSO): δ = 171.70, 171.14, 171.04, 170.89, 159.61, 155.89, 153.50, 152.96, 152.90, 138.08, 136.89, 129.20, 128.21, 128.03, 127.63, 127.42, 126.37, 126.22, 118.41, 117.50, 113.71, 110.12, 65.23 (CH_2O of Z), 56.15, 51.23, 40.68, 37.25, 29.64, 27.17, 18.17 ppm (CH_3); MS (ESI$^+$): *m/z* calcd for $C_{34}H_{34}N_3O_{10}$: 644.22 $[M+H]^+$; found: 644.3; elemental analysis calcd (%) for $C_{34}H_{33}N_3O_{10}$: C 63.45, H 5.17, N 6.53; found: C 62.10, H 5.17, N 6.46.

Fluorimetric assay

Buffer systems and TGase 2 stock solutions: For the measurements at pH 8.0 and pH 6.5, the following two assay buffers of the corresponding pH value were used.

buffer A: 3-(*N*-morpholino)propanesulfonic acid (MOPS, pH 8.0, 100 mM), $CaCl_2$ (3 mM), EDTA (50 μM), adjusted to pH 8.0 with NaOH (1 M)

buffer B: 2-(*N*-morpholino)ethanesulfonic acid (MES, pH 6.5, 100 mM), $CaCl_2$ (3 mM), EDTA (50 μM), adjusted to pH 6.5 with NaOH (1 M)

Two different enzyme buffers were used for the preparation of the TGase 2 stock solutions:

buffer I: MOPS (pH 8.0, 100 mM), $CaCl_2$ (3 mM), DTT (10 mM), glycerol (20%, *v/v*)

buffer II: MOPS (pH 8.0, 100 mM), $CaCl_2$ (3 mM), TCEP (10 mM), glycerol (20%, *v/v*)

For kinetic measurements at pH 6.5, TGase 2 stock solutions in buffer II were used; these were diluted with buffer III.

buffer III: MES (pH 6.5, 100 mM), $CaCl_2$ (3 mM), TCEP (10 mM), glycerol (20%, *v/v*)

All buffers were stored at 0 °C for periods of up to two weeks and freshly prepared after that period. The concentrations of the enzyme stock solutions were 0.5 mg mL^{-1} and 1 mg mL^{-1} for gpTGase 2 and hTGase 2, respectively.

General assay procedure and analysis: All measurements were conducted at 30 °C over 900 s (interval of 20 s) with a Synergy 4 Multi-Mode Microplate Reader (BioTek Instruments) and black 96-well BRANDplates with transparent bottoms (BRAND). Fluorescence was detected in bottom read mode. To detect released HMC or HC, a combination of optical filters adjusted to 365/40 nm and 465/40 nm as ranges of wavelengths for excitation and emission, respectively, were used. Measurements at pH 8.0 and pH 6.5 were conducted with sensitivities of 35 and 45, respectively. The assay mixture (200 μL) contained aqueous solution (190 μL) and DMSO (5%, *v/v*, 10 μL). All regression analyses were accomplished with GraphPad Prism (version 5.02, 17.12.2008). To provide values of means and SEMs, the corresponding regression analyses were separately accomplished for each experiment, and the obtained fit values were collected and statistically analysed.

Assay procedure and kinetic analysis of the enzymatic hydrolyses: For investigations on enzyme-catalysed hydrolysis reactions, six or eight different concentrations of the acyl donors were used (three independent measurements for each concentration in duplicate). The corresponding stock solutions were prepared in DMSO. DMSO (5 μL) and the acyl donor stock solution (5 μL) were added to assay buffer (180 μL). The reactions were initiated by addition of TGase 2 (10 μL, 60 μg mL^{-1}). For measurements of the spontaneous reactions, the TGase 2 solution was replaced by the appropriate enzyme buffer. The recorded time courses of type (RFU−RFU$_0$)=*f*(t) for the enzymatic conversions were analysed by nonlinear regression to the experimental data over the first 300 s by use of Equation (1) (one-phase association). Subsequently, the first derivative of this function at $t=0$ [Eq. (2)] afforded the initial slopes, which are equal to the values of $v_{0\,total}$ (units of RFU s^{-1}).

$$RFU - RFU_0 = plateau \times (1 - e^{-kt}) \quad (1)$$

RFU$_0$: RFU$_{t=0}$. Plateau: RFU$_{t\to\infty}$. *k*: rate constant to reach the plateau.

$$v_{0\,total} = k \times plateau \quad (2)$$

With regard to the measurements of compound **5b** at pH 6.5, time courses of type (RFU−RFU$_0$)=*f*(*t*) were analysed either by nonlinear [Eq. (1)] or by linear regression over the first 300 s to the experimental data, depending on the shape of the curve.

The rates for the spontaneous reactions ($v_{0\,control}$) in the absence of enzyme were determined as described below. All fluorescence rates (RFU s^{-1}) were converted into molar rates [μM min^{-1}] by dividing by the corresponding fluorescence coefficients. Subsequently, the two sets of initial rates {$v_{0\,total}=f$([acyl donor]) and $v_{0\,control}=f$([acyl donor])} were globally analysed by use of the model of total and nonspecific binding as implemented in GraphPad Prism to determine the kinetic parameters for the enzymatic conversion. Accordingly, the following rule was defined [Eq. (3)]:

$$v_{0\,total} = v_{0\,corr} + v_{0\,control} \quad (3)$$

where $v_{0\,corr}$ represents the rates for the enzymatic conversions. Within this model, the portion of $v_{0corr}=f$([acyl donor]) and $v_{0\,control}=f$([acyl donor]) were analysed by nonlinear regression by use of Equation (4) (Michaelis–Menten equation) and linear regression ($v_{0\,control}=k_{obs}$*[acyl donor]), respectively, with the data (see Figures S11 and S12 for global plots).

$$v_{0\,corr} = \frac{v_{max} \times [S]}{K_m + [S]} \quad (4)$$

Because of the negligible spontaneous reaction of compound **5b** at pH 6.5, plots of $v_{0\,total}=f$([acyl donor]) were directly analysed by nonlinear regression to the data by use of Equation (4).

Analysis of the spontaneous reactions: The recorded time courses of type (RFU−RFU$_0$)=*f*(*t*) for the spontaneous reactions were analysed by linear regression to the experimental data over the first 120 s. The respective slopes are equal to the values of $v_{0\,control}$ (units of RFU s^{-1}).

To determine the pseudo-first-order rate constants (k_{obs}), plots of $v_{0\,control}=f$([acyl donor]) were analysed by linear regression to the data. The obtained slopes are identical to the k_{obs} values.

Assay procedure and kinetic analysis of the enzymatic aminolysis: For investigations of enzyme-catalysed aminolysis reactions, six different concentrations of the acyl donors were used (three independent measurements, each concentration in duplicate). The appropriate stock solutions were prepared in DMSO. Aminoacetonitrile was chosen as reference acyl acceptor. Aminoacetonitrile in DMSO (16 mM, 5 μL) and the acyl donor stock solution (5 μL) were added to assay buffer (180 μL). The reactions were initiated by addition of TGase 2 (10 μL, 6 μg mL^{-1} for **5a**, **5b**, **6a** and **6b** or 40 μg mL^{-1} for **3** and **4**). For the measurement of the spontaneous reactions, the TGase 2 solution was replaced by the appropriate enzyme buffer. The recorded time courses of type (RFU−RFU$_0$)=*f*(*t*) for the enzymatic conversions were analysed by nonlinear regression with the experimental data over 180 s by use of Equation (1) (one-phase association). Values of $v_{0\,total}$ and $v_{0\,control}$ were obtained as described for the enzymatic hydrolysis. Because of the high rates of spontaneous and enzymatic reactions, the calculated substrate concentrations from the numerical integration were used. Finally, the two sets of initial rates ($v_{0\,total}$ and $v_{0\,control}$) were globally analysed with use of a model of total and nonspecific

binding as described for the enzymatic hydrolysis (see Figures S14 and S15 for global plots). The evaluation of the data sets for compounds **6a** and **6b** (gpTGase 2) and compound **5b** (hTGase 2) were performed by the method of Cornish-Bowden and Eisenthal.[40]

Characterisation of acyl acceptors: To characterise the kinetic properties of the chosen acyl acceptor substrates [aminoacetonitrile and *N*-(biotinyl)cadaverine (**7**)·TFA] six different concentrations of the acyl acceptors were used. The appropriate stock solutions were prepared in DMSO. Compound **5b** was chosen as acyl donor. Acyl acceptor stock solution (5 μL) and **5b** in DMSO (4 mM, 5 μL) were added to assay buffer (180 μL). The reactions were initiated upon addition of TGase 2 (12 μg mL^{-1}, 10 μL). For measurement of the spontaneous reactions, the TGase 2 solution was replaced by the appropriate enzyme buffer. The two sets of initial rates ($v_{0\,\mathrm{total}}$ and $v_{0\,\mathrm{control}}$) were obtained as described for the enzymatic hydrolysis. Subsequently, the $v_{0\,\mathrm{control}}$ values were subtracted from the corresponding $v_{0\,\mathrm{total}}$ values, and the resulting plot of $v_{0\,\mathrm{corr}}=f([S])$ was analysed by use either of Equation (4) for aminoacetonitrile or of Equation (5) for *N*-(biotinyl)cadaverine (**7**).

$$v_{0\,\mathrm{corr}} = \frac{v_{\max} \times [S]}{K_m + [S] \times (1 + [S]/K_i)} \quad (5)$$

Because the measurements with *N*-(biotinyl)cadaverine (**7**) required highly concentrated amine stock solutions (400 mM), the volumes of the stock solutions were significantly greater than that of the added DMSO for dissolving the compounds, due to the large amount of amine, which finally resulted in lower concentrations than intended. Therefore, the applied concentrations had to be corrected. For this purpose, the density of the appropriate stock solution was determined by weighing a defined volume, and the correct concentration was calculated by using the obtained density and the overall weight of the solution (DMSO + amine). The ratio between the actual and the intended concentration of the stock solution provided a factor (0.94) that was then used to correct the concentrations of all other solutions made from the stock solution.

Inhibition experiments: For the characterisation of coumarinyl amide **5c** with gpTGase 2 at pH 8.0, the enzymatic hydrolysis of **5b** in the presence of four concentrations of **5c** (0, 200, 300 and 500 μM) was recorded. The corresponding stock solutions of **5b** and **5c** were prepared in DMSO. Stock solution of **5c** (5 μL) and stock solution of **5b** (5 μL) were added to assay buffer (180 μL). The reactions were initiated upon addition of gpTGase 2 (60 μg mL^{-1}, 10 μL). For the measurement of the spontaneous reactions, the TGase 2 solution was replaced by the appropriate enzyme buffer. Data evaluation was carried out as described in the Supporting Information (Discussion S7).

For the characterisation of iodoacetamide and acrylamide **8** with gpTGase 2 and hTGase 2 at pH 6.5, eight or six concentrations of the inhibitors were used. The appropriate stock solutions were prepared in DMSO. Compound **5b** was chosen as acyl donor. Iodoacetamide stock solution (5 μL) and either **5b** (1 mM, for gpTGase 2) or **5b** (1.2 mM, 5 μL, for hTGase 2) in DMSO were added to assay buffer (180 μL). The reactions were initiated upon addition of TGase 2 (60 μg mL^{-1}, 10 μL). The recorded time courses of type $(RFU-RFU_0)=f(t)$ were analysed by nonlinear regression with the experimental data over the entire measurement period (900 s) by use of Equation (6):

$$RFU-RFU_0 = v_s \times t + \frac{(v_i - v_s)(1-e^{-k_{obs}t})}{k_{obs}} \quad (6)$$

v_s: steady-state velocity. v_i: initial velocity.

For iodoacetamide (gpTGase 2 and hTGase 2) and acrylamide **8** (gpTGase 2), the plot of $k_{obs}=f([I])$ was analysed by linear regression to the data. The corresponding slope (k_{obs}/I) was converted into k_{inact}/K_I by multiplication [Eq. (7)] by $(1+[S]/K_m)$. For the inhibition of hTGase 2 by acrylamide **8**, the double reciprocal plot $1/k_{obs}=f([1/[I])$ [Eq. (8)] was analysed by linear regression to the data to determine the values for k_{incat}, K_I and k_{inact}/K_I. The appropriate K_i value was determined by analysis of $v_i=f([I])$ by use of Equation (9) and the equation $K_i=K_i'/(1+[S]/K_m)$, with $K_m=6.60$ μM.

$$k_{obs} = \frac{k_{inact} \times [I]}{K_I + [I]} \quad (7)$$

$$\frac{1}{k_{obs}} = \frac{K_I}{k_{inact}} \times \frac{1}{[I]} + \frac{1}{k_{inact}} \quad (8)$$

$$v_i = \frac{v_0}{1 + [I]/K_i'} + v_{0\,\mathrm{control}} \quad (9)$$

Numerical integration: For analysis of progress curves $[RFU=f(t)]$ by numerical integration the differential equations shown in Scheme 5 and Scheme 7 were implemented in the freely available software R (www.r-project.org/). A series of parameters were also implemented: fluorescent coefficients of HMC or HC (coP), the acyl donors (coSL) and the background fluorescence (bg), active concentrations of TGase 2, the rate constants k_{obs} for spontaneous reactions of the acyl donors, time span between data points (20 s), the entire time period for analysis (same as for the analysis by nonlinear regression) and starting values for the concentrations of the acyl donors and inhibitors. These parameters had to be defined depending on the data set prior to performing numerical integration. Furthermore, the following relations were also implemented:

Enzymatic hydrolysis and aminolysis:

$$k_{-1} = k_1 \times K_m - k_{cat}$$

where k_1 was kept constant at the assumed value of 1 μM^{-1} s^{-1}

$$RFU = coP \times [P] + coSL \times [SL] + bg$$

For fitting of the progress curves, the kinetic parameters K_m and k_{cat} obtained by nonlinear regression or by the method of Cornish-Bowden and Eisenthal were used as initial values.

Enzymatic hydrolysis in the presence of an irreversible inhibitor:

$$k_1 = \frac{k_{-1} + k_{cat}}{K_m}$$

where k_{-1} was kept constant at the assumed value of 1 s^{-1}

$$k_2 = \frac{k_{-2} + k_{inact}}{K_I}$$

where k_{-2} was kept constant at the assumed value of 1 s^{-1}

$$k_{inact} = r \times K_I$$

thus $r=k_{inact}/K_I$

$$RFU = coP \times [P] + coSL \times [SL] + bg$$

The value of k_{inact}/K_I obtained by regression analysis was used as initial value for r, and an arbitrary value of $K_I = 15$ μM was set. Therefore, this procedure only allowed for the reliable calculation of the second-order inactivation constant k_{inact}/K_I. Each experiment was fitted separately, and final values of means ±SEMs shown in Tables 2 and 3 were calculated by statistical analysis of all experiments.

Presetting of the parameters above to arbitrarily assumed values was necessary because the rate constants describing the reversible enzyme·substrate and enzyme·inhibitor complexes cannot be calculated independently.[33]

Acknowledgements

*The authors thank Elisabeth Jäckel and Martin Lohse (Helmholtz-Zentrum Dresden–Rossendorf, Institute of Radiopharmaceutical Cancer Research) for assisting in the synthesis of compound **8** and **5c**, respectively, and are grateful to Gözde Sarican (Trakya University, Edirne, Turkey, financially supported by a scholarship within the Erasmus programme for residence at the University of Cologne) for initial investigations into compounds **2a**–**2c**. R.L. appreciates continuing support by Prof. Dr. Jörg Steinbach. Partial financial support by the Helmholtz Portfolio Topic "Technologie und Medizin—Multimodale Bildgebung zur Aufklärung des in vivo-Verhaltens von polymeren Biomaterialien" (R.W., J.P. and R.L.) and by the Fonds der Chemischen Industrie (R.L.) is gratefully acknowledged. Furthermore, we wish to thank Prof. Dr. Jörg van den Hoff for helpful discussions concerning numerical integration.*

Keywords: enzyme assays · inhibitors · reactive peptides · solid-phase synthesis · transferases

[1] a) G. W. Jameson, D. V. Roberts, R. W. Adams, W. S. A. Kyle, D. T. Elmore, *Biochem. J.* **1973**, *131*, 107–117; b) S. P. Leytus, L. L. Melhado, W. F. Mangel, *Biochem. J.* **1983**, *209*, 299–307; c) J. L. Reymond, V. S. Fluxa, N. Maillard, *Chem. Commun.* **2009**, 34–46; d) S. S. van Berkel, B. van der Lee, F. L. van Delft, R. Wagenvoord, H. C. Hemker, F. P. Rutjes, *ChemMedChem* **2012**, *7*, 606–617; e) M. Sakabe, D. Asanuma, M. Kamiya, R. J. Iwatate, K. Hanaoka, T. Terai, T. Nagano, Y. Urano, *J. Am. Chem. Soc.* **2013**, *135*, 409–414; f) M. Prost, L. Canaple, J. Samarut, J. Hasserodt, *ChemBioChem* **2014**, *15*, 1413–1417; g) K. R. Tallman, K. E. Beatty, *ChemBioChem* **2015**, *16*, 70–75; h) A. Zadlo, D. Koszelewski, F. Borys, R. Ostaszewski, *ChemBioChem* **2015**, *16*, 677–682.

[2] a) D. Park, S. S. Choi, K. S. Ha, *Amino Acids* **2010**, *39*, 619–631; b) S. Gundemir, G. Colak, J. Tucholski, G. V. Johnson, *Biochim. Biophys. Acta Mol. Cell Res.* **2012**, *1823*, 406–419; c) R. L. Eckert, M. T. Kaartinen, M. Nurminskaya, A. M. Belkin, G. Colak, G. V. Johnson, K. Mehta, *Physiol. Rev.* **2014**, *94*, 383–417.

[3] a) N. K. Sarkar, D. D. Clarke, H. Waelsch, *Biochim. Biophys. Acta* **1957**, *25*, 451–452; b) M. J. Mycek, D. D. Clarke, A. Neidle, H. Waelsch, *Arch. Biochem. Biophys.* **1959**, *84*, 528–540; c) J. Schrode, J. E. Folk, *J. Biol. Chem.* **1978**, *253*, 4837–4840.

[4] M. J. Mycek, H. Waelsch, *J. Biol. Chem.* **1960**, *235*, 3513–3517.

[5] a) P. A. Smethurst, M. Griffin, *Biochem. J.* **1996**, *313*, 803–808; b) N. S. Caron, L. N. Munsie, J. W. Keillor, R. Truant, *PLoS One* **2012**, *7*, e44159; c) M. S. Pavlyukov, N. V. Antipova, M. V. Balashova, M. I. Shakhparonov, *Biochem. Biophys. Res. Commun.* **2012**, *421*, 773–779.

[6] a) H. Nakaoka, D. Perez, K. Baek, T. Das, A. Husain, K. Misono, M. Im, R. Graham, *Science* **1994**, *264*, 1593–1596; b) S. S. Akimov, D. Krylov, L. F. Fleischman, A. M. Belkin, *J. Cell Biol.* **2000**, *148*, 825–838; c) A. M. Belkin, *FEBS J.* **2011**, *278*, 4704–4716.

[7] a) W. Dieterich, T. Ehnis, M. Bauer, P. Donner, U. Volta, E. O. Riecken, D. Schuppan, *Nat. Med.* **1997**, *3*, 797–801; b) A. Di Sabatino, A. Vanoli, P. Giuffrida, O. Luinetti, E. Solcia, G. R. Corazza, *Autoimmun. Rev.* **2012**, *11*, 746–753; c) C. Klöck, T. R. DiRaimondo, C. Khosla, *Semin. Immunopathol.* **2012**, *34*, 513–522.

[8] a) L. Elli, C. M. Bergamini, M. T. Bardella, D. Schuppan, *Dig. Liver Dis.* **2009**, *41*, 541–550; b) D. Caccamo, M. Curro, R. Ientile, *Expert Opin. Ther. Targets* **2010**, *14*, 989–1003; c) K. C. Olsen, R. E. Sapinoro, R. M. Kottmann, A. A. Kulkarni, S. E. Iismaa, G. V. Johnson, T. H. Thatcher, R. P. Phipps, P. J. Sime, *Am. J. Respir. Crit. Care Med.* **2011**, *184*, 699–707.

[9] a) H. Grosso, M. M. Mouradian, *Pharmacol. Ther.* **2012**, *133*, 392–410; b) A. C. Brett, T. R. Rosenstock, A. C. Rego, *Curr. Drug Targets* **2014**, *15*, 313–334; c) R. Ientile, M. Curro, D. Caccamo, *Amino Acids* **2015**, *47*, 19–26.

[10] a) P. Kotsakis, M. Griffin, *Amino Acids* **2007**, *33*, 373–384; b) K. Mehta, A. Kumar, H. I. Kim, *Biochem. Pharmacol.* **2010**, *80*, 1921–1929; c) S. Kumar, K. Mehta, *Amino Acids* **2013**, *44*, 81–88.

[11] M. Pietsch, R. Wodtke, J. Pietzsch, R. Löser, *Bioorg. Med. Chem. Lett.* **2013**, *23*, 6528–6543.

[12] S. M. Gillet, J. N. Pelletier, J. W. Keillor, *Anal. Biochem.* **2005**, *347*, 221–226.

[13] M. Walker, *Top. Med. Chem.* **2015**, *9*, 69–106.

[14] J. Wityak, M. E. Prime, F. A. Brookfield, S. M. Courtney, S. Erfan, S. Johnsen, P. D. Johnson, M. Li, R. W. Marston, L. Reed, D. Vaidya, S. Schaertl, A. Pedret-Dunn, M. Beconi, D. Macdonald, I. Muñoz-Sanjuan, C. Dominguez, *ACS Med. Chem. Lett.* **2012**, *3*, 1024–1028.

[15] M. Dixon, E. C. Webb, C. J. R. Thorne, K. F. Tipton, *Enzymes*, Academic Press, New York, **1979**, pp. 78–79.

[16] J. Polster, *Reaktionskinetische Auswertung spektroskopischer Meßdaten*, Vieweg, Braunschweig, **1995**, pp. 80–115.

[17] F. García-Martín, N. Bayó-Puxan, L. J. Cruz, J. C. Bohling, F. Albericio, *QSAR Comb. Sci.* **2007**, *26*, 1027–1035.

[18] J. D. K. Twibanire, T. B. Grindley, *Org. Lett.* **2011**, *13*, 2988–2991.

[19] R. Bollhagen, M. Schmiedberger, K. Barlos, E. Grell, *J. Chem. Soc. Chem. Commun.* **1994**, 2559–2560.

[20] a) S. I. Chung, R. I. Shrager, J. E. Folk, *J. Biol. Chem.* **1970**, *245*, 6424–6435; b) A. Leblanc, C. Gravel, J. Labelle, J. W. Keillor, *Biochemistry* **2001**, *40*, 8335–8342.

[21] a) W. P. Jencks, J. Carriuolo, *J. Am. Chem. Soc.* **1960**, *82*, 1778–1786; b) O. S. Tee, O. J. Yazbeck, *Can. J. Chem.* **2000**, *78*, 1100–1108; c) C. Gravel, D. Lapierre, J. Labelle, J. W. Keillor, *Can. J. Chem.* **2007**, *85*, 164–174.

[22] a) P. J. Bracher, P. W. Snyder, B. R. Bohall, G. M. Whitesides, *Origin Life Evol. Biosph.* **2011**, *41*, 399–412; b) Z. P. Gates, J. R. Stephan, D. J. Lee, S. B. H. Kent, *Chem. Commun.* **2013**, *49*, 786–788.

[23] a) M. J. Selwyn, *Biochim. Biophys. Acta* **1965**, *105*, 193–195; b) A. Baici, *Kinetics of Enzyme–Modifier Interactions*, Springer, Vienna, **2015**, pp. 1–64.

[24] R. A. Copeland, *Enzymes: A Practical Introduction to Structure, Mechanism, and Data Analysis*, Wiley, Hoboken, **2000**, pp. 109–145.

[25] a) D. E. Koshland, *Bioorg. Chem.* **2002**, *30*, 211–213; b) R. Eisenthal, M. J. Danson, D. W. Hough, *Trends Biotechnol.* **2007**, *25*, 247–249.

[26] J. E. Folk, P. W. Cole, *J. Biol. Chem.* **1965**, *240*, 2951–2960.

[27] M. Griffin, A. Mongeot, R. Colligan, R. E. Saint, R. A. Jones, I. G. Coutts, D. L. Rathbone, *Bioorg. Med. Chem. Lett.* **2008**, *18*, 5559–5562.

[28] M. Malešević, A. Migge, T. C. Hertel, M. Pietzsch, *ChemBioChem* **2015**, *16*, 1169–1174.

[29] V. Gentile, M. Saydak, E. A. Chiocca, O. Akande, P. J. Birckbichler, K. N. Lee, J. P. Stein, P. J. A. Davies, *J. Biol. Chem.* **1991**, *266*, 478–483.

[30] C. Hauser, R. Wodtke, R. Löser, M. Pietsch, *Amino Acids* **2016**, DOI: 10.1007/s00726-00016-02192-00725.

[31] I. Roy, O. Smith, C. M. Clouthier, J. W. Keillor, *Protein Expression Purif.* **2013**, *87*, 41–46.

[32] a) A. Case, R. L. Stein, *Biochemistry* **2003**, *42*, 9466–9481; b) J. W. Keillor, C. M. Clouthier, K. Y. Apperley, A. Akbar, A. Mulani, *Bioorg. Chem.* **2014**, *57*, 186–197.

[33] A. Baici in *Proteases: Structure and Function* (Eds.: K. Brix, W. Stöcker), Springer, Vienna, **2013**, pp. 37–84.

[34] H. Tsunematsu, H. Nishimura, K. Mizusaki, S. Makisumi, *J. Biochem.* **1985**, *97*, 617–623.

[35] a) K. Hardes, G. L. Becker, M. Z. Hammamy, T. Steinmetzer, *Anal. Biochem.* **2012**, *428*, 73–80; b) K. Hardes, M. Zouhir Hammamy, T. Steinmetzer, *Anal. Biochem.* **2013**, *442*, 223–230.

[36] A. Baici, *Kinetics of Enzyme-Modifier Interactions*, Springer, Vienna, **2015**, pp. 127 – 169.
[37] M. C. Yi, B. A. Palanski, S. A. Quintero, N. M. Plugis, C. Khosla, *Bioorg. Med. Chem. Lett.* **2015**, *25*, 4922 – 4926.
[38] R. L. Stein, *Kinetics of Enzyme Action: Essential Principles for Drug Hunters*, Wiley, Hoboken, **2011**, pp. 141 – 168.
[39] J. E. Folk, *J. Biol. Chem.* **1969**, *244*, 3707 – 3713.
[40] A. Cornish-Bowden, *Fundamentals of Enzyme Kinetics*, Wiley-Blackwell, Oxford, **2012**, pp. 45 – 51.
[41] a) R. Eisenthal, A. Cornish-Bowden, *Biochem. J.* **1974**, *139*, 715 – 720; b) R. Eisenthal, A. Cornish-Bowden, *Biochem. J.* **1974**, *139*, 721 – 730; c) A. Baici, *Biochemist* **2006**, *28*, 36 – 39.
[42] a) T. F. Slaughter, K. E. Achyuthan, T. S. Lai, C. S. Greenberg, *Anal. Biochem.* **1992**, *205*, 166 – 171; b) J.-H. Jeon, C.-W. Kim, D.-M. Shin, K.-i. Kim, S.-Y. Cho, J.-C. Kwon, K.-H. Choi, H.-S. Kang, I.-G. Kim, *FEBS Lett.* **2003**, *534*, 180 – 184; c) X. Jin, J. Stamnaes, C. Klöck, T. R. DiRaimondo, L. M. Sollid, C. Khosla, *J. Biol. Chem.* **2011**, *286*, 37866 – 37873.
[43] M. T. Gundersen, J. W. Keillor, J. N. Pelletier, *Appl. Microbiol. Biotechnol.* **2014**, *98*, 219 – 230.
[44] A. Cornish-Bowden, *Fundamentals of Enzyme Kinetics*, Wiley-Blackwell, Oxford, **2012**, pp. 211 – 213.
[45] R. L. Stein, *Kinetics of Enzyme Action: Essential Principles for Drug Hunters*, Wiley, Hoboken, **2011**, pp. 122 – 137.
[46] R. A. Copeland, *Evaluation of Enzyme Inhibitors in Drug Discovery*, Wiley, Hoboken, **2005**, pp. 214 – 248.
[47] J. E. Folk, P. W. Cole, *J. Biol. Chem.* **1966**, *241*, 3238 – 3240.
[48] A. G. McDonald, K. F. Tipton in *eLS*, Wiley, Chichester, **2012**, pp. 1 – 17.
[49] C. Cobas, S. Dominguez, N. Larin, I. Iglesias, C. Geada, F. Seoane, M. Sordo, P. Monje, S. Fraga, R. Cobas, C. Peng, J. A. Garcia, M. Goebel, E. Vaz, *MestReNova 6.1.1 – 6384*, Mestrelab Research S. L., **2010**.

Manuscript received: January 25, 2016
Accepted article published: April 28, 2016
Final article published: ■■ ▮▮, 0000

R. Wodtke, G. Schramm, J. Pietzsch, M. Pietsch, R. Löser**

■■ – ■■

Synthesis and Kinetic Characterisation of Water-Soluble Fluorogenic Acyl Donors for Transglutaminase 2

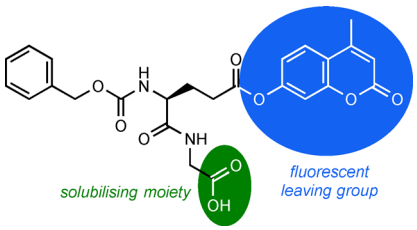

Fluorimetric assay for Transglutaminase 2: A set of fluorogenic acyl donor substrates for transglutaminase 2 was synthesised by a modular solid-phase strategy. Their good aqueous solubility allowed for a detailed kinetic characterisation with regard to their TGase 2-catalysed hydrolysis and aminolysis. Their applicability to characterising amine substrates and inhibitors of TGase 2 was also demonstrated.